ADVANCES IN NORTH AMERICAN AVALANCHE TECHNOLOGY: 1972 Symposium

USDA Forest Service General
Technical Report RM-3

September 1973

Rocky Mountain Forest and
Range Experiment Station

Forest Service

U.S. Department of Agriculture

Fort Collins, Colorado 80521

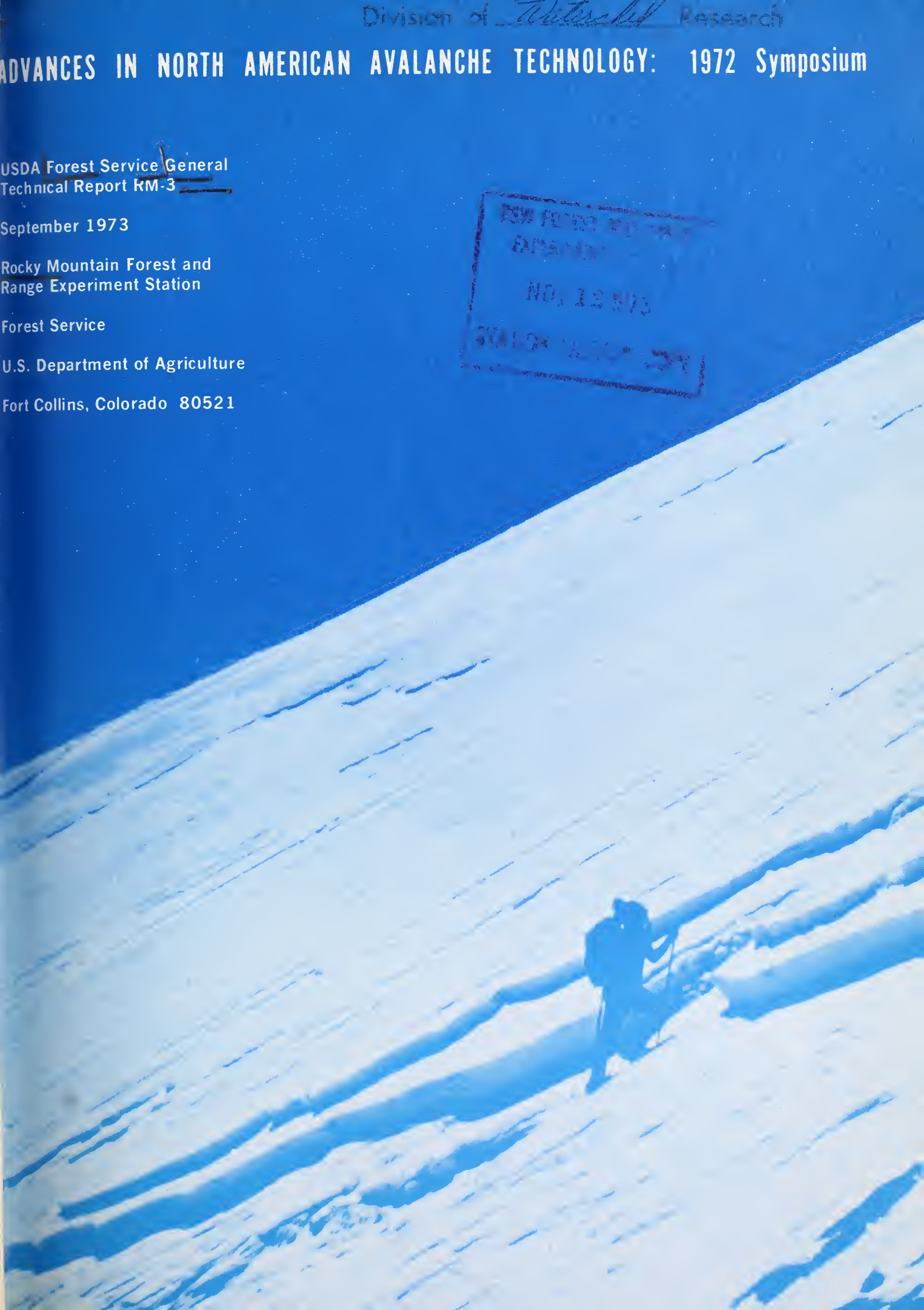

ABSTRACT

Seven technical presentations, made in connection with the USDA Forest Service National Avalanche Training Program, discuss acoustic signals emitted by snow under stress, aspects of snow slab mechanics, use of explosives, and problems of avalanche dynamics.

Oxford: 384.1:111.784. **Keywords:** Avalanches, snow management.

USDA Forest Service
General Technical Report RM-3

September 1973

ADVANCES IN NORTH AMERICAN AVALANCHE TECHNOLOGY: 1972 SYMPOSIUM

Compiled by

R. I. Perla

Alpine Snow and Avalanche Project
Rocky Mountain Forest and Range Experiment Station[1]

Technical presentations made in connection with the USDA Forest Service National Avalanche Training Program, Reno, Nevada, November 16-17, 1972

[1]*Central headquarters is maintained in cooperation with Colorado State University, Fort Collins.*

ADVANCES IN NORTH AMERICAN AVALANCHE TECHNOLOGY: 1972 SYMPOSIUM

PREFACE

As part of its National Avalanche Training Program, the USDA Forest Service hosted a symposium at Reno, Nevada, on November 16 and 17, 1972. The symposium, arranged by R. I. Perla and R. H. Spray, was chaired by E. R. LaChapelle. Seven of the technical presentations are published herein.

The opening contribution by W. St. Lawrence and C. Bradley reports on acoustic signals emitted by snow under stress. One exciting breakthrough is mentioned — the discovery of the Kaiser acoustic effect in snow. St. Lawrence and Bradley envision that acoustic emission phenomena, including the Kaiser effect, may have important applications for testing the structural integrity of avalanche slopes.

The next four contributions discuss various aspects of snow slab mechanics. This research is motivated by needs of the ski industry to control the slab avalanche problem. Reading these papers, one may conclude that snow slab mechanics is a young, wide-open subject. There is still much speculation on the release mechanisms of slab avalanches, and the stage is set for some convincing experiments.

Since the basic mechanics of slab release are unknown, many uncertainties exist about how to artificially release slab avalanches with explosives. The paper by M. Mellor is a bold start in explaining how explosives can be used rationally and systematically in avalanche technology.

Research effort in the United States has centered around slab-stability investigations; Canadian research, however, has looked into the problems of avalanche dynamics. In a brief, significant report, P.A. Schaerer presents a very practical way of computing impact pressure of moving avalanches.

R. I. Perla, Compiler

CONTENTS

ULTRASONIC EMISSIONS IN SNOW

William St. Lawrence and Charles Bradley

ABSTRACT

Burst type acoustic signals have been monitored in snow subjected to various load and deformation histories over a wide range of frequencies. The pattern of the acoustic response is closely related to the particular load or deformation history applied. Examination of the emission pattern suggests a description of the deformation of snow in terms of a structural mechanism. The results of a number of experiments are given and interpreted in terms of their acoustic response.

Also presented is a discussion of the possible application of the acoustic emission technique for making *in situ* measurements of the state of stress in an active snow slope.

Introduction

A number of different types of acoustic signals which emanate from snow subjected to mechanical loadings have been detected. These signals can be broadly classified into two groups: audible and subaudible. In terms of audible signals we can cite such examples as the squeaking which can often be heard when walking on snow on a cold day, or the sharp report which accompanies a rapidly propagating crack in the tensile region of a snow slope. Less familiar examples of audible sounds that can be detected in snow are the sound of a collapsing snowpack, and the sound of one layer of snow slipping over an adjacent layer.

The second category, subaudible noise, can be subdivided into frequency related classifications. In one instance the sound is in the audible spectrum, but is of such low intensity that it cannot be detected by the unaided ear. To date we have detected this type of signal only in snow samples subjected to deformation rates which induce a brittle response in the snow. The second type of noise is ultrasonic. This type of acoustic emission has been monitored in snow over a wide range of loadings. It is this kind of emission that will be dealt with in this paper.

Emission Characteristics and Possible Sources

To investigate the nature of ultrasonic emissions in snow, consideration must be given to the possible source of the acoustic event, and to the system used for detecting it. Consideration of the acoustic emission monitoring system, and in particular the transducer, is important since information obtained in terms of frequency content, amplitude, and duration of an acoustic event in general reflect system characteristics. The source disturbances probably bear little resemblance to the signal that is recorded. In defining ultrasonic emissions we are indicating that the transducer used is most sensitive to excitation in the ultrasonic region of the frequency spectrum.

Since the energy release associated with a burst emission is small (an estimate in the neighborhood of 10^{-13} Joules has been suggested by Liptai et al. 1971), it is customary to monitor the transducer used to detect the acoustic signal in the vicinity of one of its resonance peaks. This method makes it possible to detect small amplitude signals, but provides little information about the form of the exciting signal. Using this technique limits the information obtained to establishing a transient disturbance has taken place, and that the disturbance has sufficient energy in the region of the transducer resonant frequency to excite the transducer to resonance. A definite advantage in working in the ultrasonic region of the frequency spectrum is that for frequencies above 30 KHz interference from extraneous noise is minimal.

As indicated above, it is difficult to describe in any detail or with any precision the form of the acoustic emission as it originates. The fact that acoustic signals are detected in snow indicates that when snow is subjected to mechanical loadings, a nonconservative energy conversion takes place, with part of this energy being dissipated in the form of noise.

It is probably correct to assume that acoustic energy represents only a small portion of the total energy dissipated. From oscilloscope and magnetic tape records we can establish that the emission of sound from snow occurs in bursts of noise rather than continuously. These bursts take place at intermittent intervals depending on the particular loading applied.

To identify the sources of acoustic emissions in snow we will rely on observations that have been made of the structural changes that take place in snow during the deformation process. From these observations we can tentatively identify possible emission sources. For deformation rates which produce a brittle response in the snow, Kinosita (1967) observes that failure is characterized by the breaking of bonds between ice crystals composing the snow matrix. For this type of deformation we detect both ultrasonic and audio signals emanating from the snow. Since Kinosita indicates that intercrystalline fracture is the only means by which snow deforms at high rates we are probably correct in assuming that for these rates some form of intergranular movement generates the acoustic signal observed.

For snow that is deformed at rates which produce a plastic response, acoustic emissions may be due to a number of different mechanisms. Observations reported by Wakahama (1967) on the compression of snow at slow rates indicate that the structural changes which take place in the snow matrix are basal glide, slip at grain boundaries and separation of ice grains. It appears plausible that accoustic emissions can originate from the formation of slip planes in the ice grains and also from the separation of ice grains. In the case of the formation of the slip plane this takes place at a rapid rate in the ice grain. A number of these slip planes forming simultaneously in the ice crystals comprising the snow matrix might produce an acoustic signal at a level that can be detected. If the separation of ice grains takes place in a rapid manner this may also represent an acoustic source. In the case of slipping at grain boundaries it would appear that this kind of process would not generate sufficient power to produce a detectable acoustic signal. Wakahama also reports that in addition to these primary mechanisms grain fracture, void formation, and grain boundary migrations are also observed. In considering these mechanisms as possible acoustic sources it is probable that grain fracture and the formation of voids within grains could generate transient acoustic signals. A number of experiments are now being planned which will attempt to look at each of the above mechanisms as possible emission sources; one that is presently being considered on a theoretical basis is the form of the stress wave which might emanate from these mechanisms.

Acoustic Emission Monitoring System

The experimental system which is used to monitor and record acoustic emissions in snow, in the laboratory, is shown schematically in figure 1. This system is typical of many acoustic emission systems presently employed for work in materials research. Since the basic acoustic emission system is well described in the literature, the reader is referred to papers by Tatro (1971) and Dunegan and Harris (1969) for complete details. It is worth commenting on a special modification that is necessary when working with snow.

Since snow is a soft material, mounting the transducer to the snow poses two special problems. Care must be taken so that spurious stress fields are not set up by having the transducer come in direct contact with the snow. Also, many tests are conducted at relatively high rates and to large deformations, so that it is possible to generate pseudo-emissions caused by the relative motion between the specimen and the transducer. Both of these problems are solved by applying a thick coating of silicon grease to the transducer so that it is not in direct contact with the snow sample.

The system used in our present experiments records only the rate at which emissions occur and the total number of emissions.

Experimental Results

In order to establish baseline data on acoustic emissions in snow, we conducted a series of experiments in which a number of load and deformations were applied. These experiments consisted of constant rate tests in tension, compression, and torsion and creep tests in tension and compression. The snow used in these experiments can best be classified as IIB2, using the classification system of Sommerfeld and LaChapelle (1970).

Figure 2 depicts a typical emission response curve (rate of emission vs. time) for a sample of snow subjected to a constant rate of deformation. The stress time curve for this test is also shown. The snow in this test was deformed at a constant angular rate of 2.2° per minute (0.12° per minute per centimeter of length.) for 20 minutes and allowed to relax for 10 minutes. At the end of the 10-minute relaxation period, the specimen was then reloaded at the same rate. The results obtained when the specimen was reloaded are also shown. The stress response curve is for the shear stress calculated at the specimens outer radius. The acoustic response depicted here is typical of the results obtained for snow subject to constant deformation rates, with variations

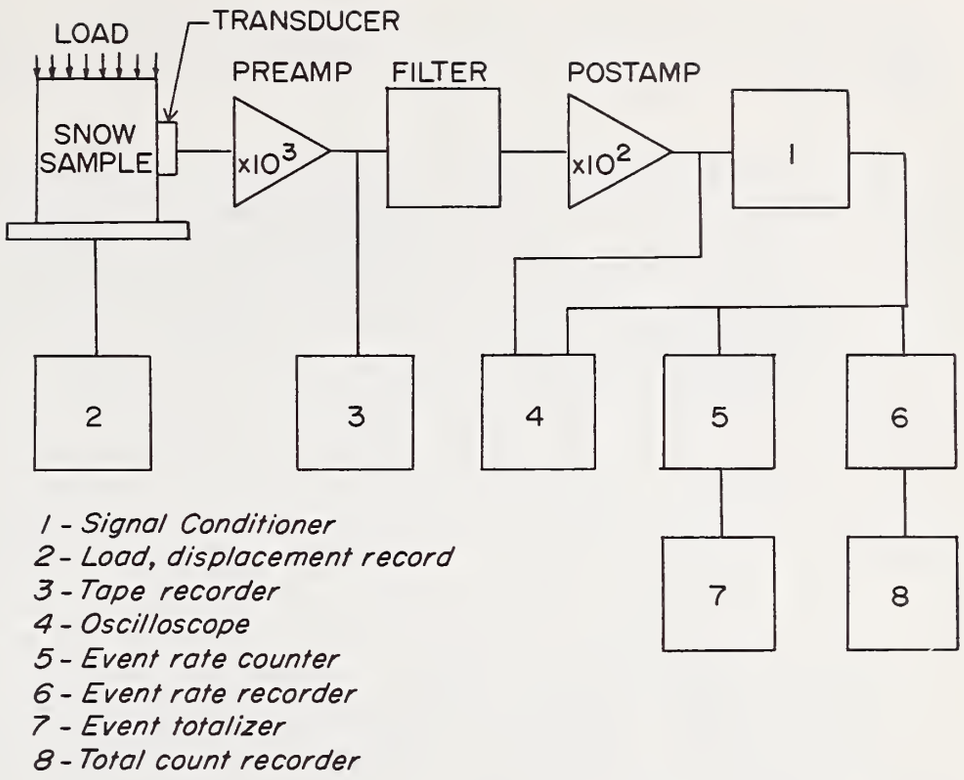

Figure 1. Acoustic emission monitoring system for snow.

1 - Signal Conditioner
2 - Load, displacement record
3 - Tape recorder
4 - Oscilloscope
5 - Event rate counter
6 - Event rate recorder
7 - Event totalizer
8 - Total count recorder

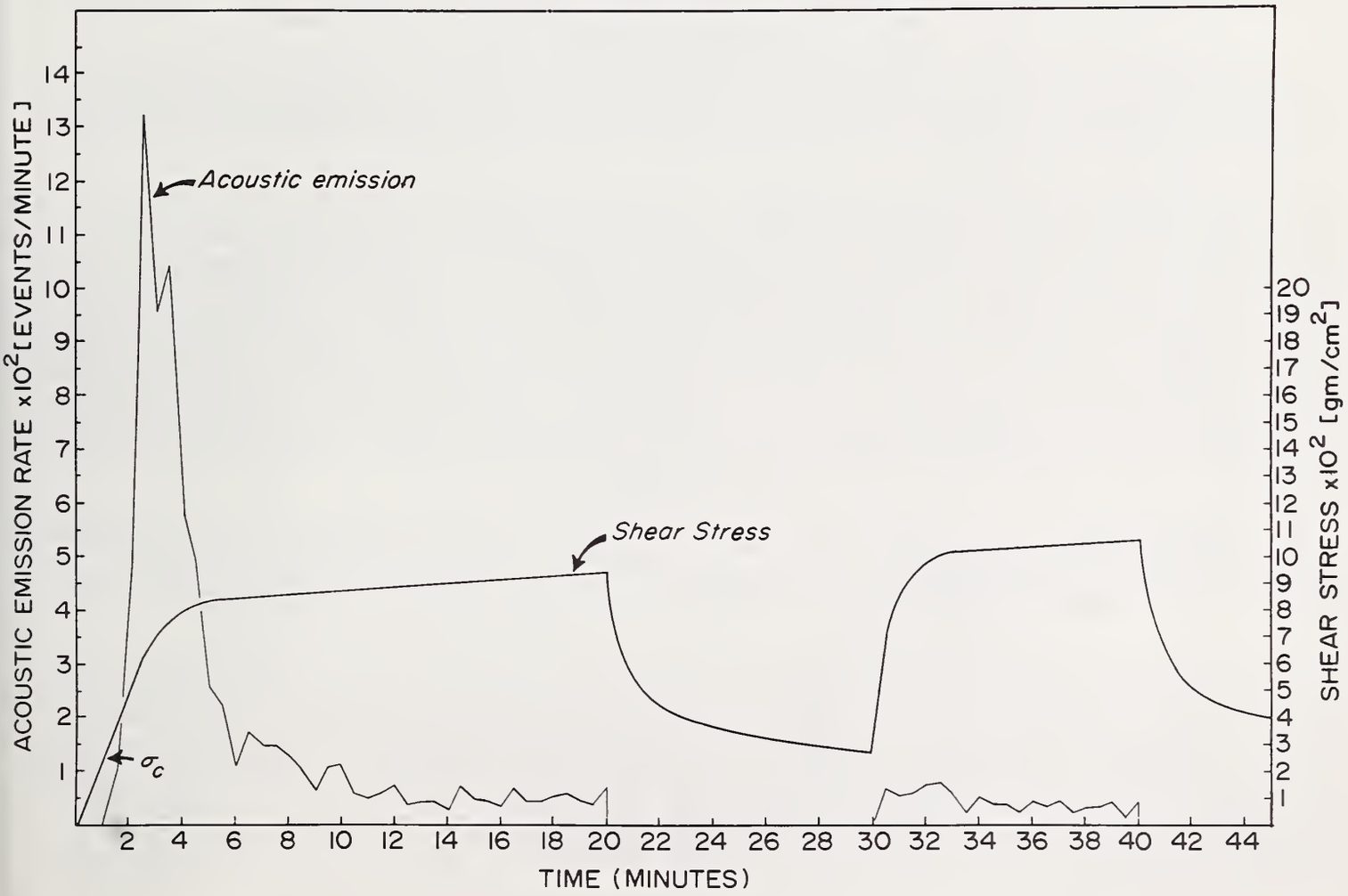

Figure 2. Acoustic emission rate response and shear stress response vs. time for a snow specimen deformed at a constant angular deformation rate of 2.2° per minute. The specimen was deformed for 20 minutes, allowed to relax for 10 minutes, and reloaded. Shear stress is calculated at the outer radius of the specimen.

being observed depending on the rate and mode of deformation (tension, compression, or torsion). Figure 2 will serve to point out the salient features of the emission response for this type of load history.

The snow used in these experiments was obtained from a collection area on relatively flat ground at a depth of about 1 meter. On this basis we will assume that the maximum stress that it had previously experienced was an overburden stress of 35 gm/cm^2. This fact is significant since prior load history is an important parameter in terms of acoustic response. As loading is initiated no acoustic response is observed until the stress reaches a certain level; this is depicted as σ_c in figure 2. As the stress increases above this value acoustic activity is initiated. The rate of acoustic activity then increases to a maximum which corresponds to the point in the stress deflection curve where the stress begins to fall off rapidly. With further deformation the rate of acoustic activity decreases steadily as the stress raches a steady state response. If the deformation is stopped, the acoustic activity ceases and the stress relaxes. If after a period of relaxation the snow is again subjected to further deformation at the same rate, the acoustic activity resumes at a rate nearly equal to what it was before deformation was terminated. This phenomenon has been observed for relaxation periods of up to 15 hours, which is the longest time that we have allowed specimens to relax before reloading. As indicated earlier, the basic acoustic emission response is similar for the three modes of deformation studied.

The acoustic emission response is very sensitive to the rate at which the snow is deformed. For relatively high rates of deformation, (that is rates close to those which induce fracture in the snow) the rate of emission rises to its maximum value and then decreases rapidly with continued deformation. Figure 2 shows the typical emission response for a high deformation rate. For very low deformation rates (rates several orders of magnitude below those which induce fracture) the acoustic emission rate curve does not show this rapid rise and decay. This rapid rise and decay feature becomes increasingly pronounced as the rate of deformation is increased.

In addition to constant deformation rate experiments a number of constant load tests in uniaxial compression and tension have been conducted and the acoustic response monitored. Figure 3a shows the acoustic response recorded for a snow sample subjected to a number of discreet load steps in uniaxial compression.

The acoustic response that is observed in creep experiments can be described as follows. For low stresses, below approximately 100 gm/cm^2 no emission activity is detected except for a few bursts when the load is initially applied. If the stress is increased an incremental amount, to a level where activity is detected, acoustic emissions are observed throughout the region of primary creep. As the creep rate approaches a steady state the rate of acoustic activity decreases to a near zero value. Again it is important to emphasize that the snow used here was subjected to only overburden stresses prior to testing. Figure 3b shows the results of unloading the above specimen, allowing it to relax and then reloading it. Note that little or no acoustic activity is observed until the stress applied to the specimen is equal to or greater than the maximum stress it had previously experienced. This interesting phenomenon is known as the Kaiser Effect, and may have a possible application for measuring the state of stress in a snowslope.

Like the constant deformation rate the basic pattern of acoustic emission tends to be similar for both tension and compression at relatively low stresses. A number of tension creep tests have been conducted at relatively high stresses (stresses in the vicinity of 500 gm/cm^2) with some interestering results being observed. The results of one such test is reported here.

A specimen was incrementally loaded over a 100-minute time interval to a stress of 500 gm/cm^2 and the acoustic response observed. Within a minute after the load was applied to produce this stress in the specimen, the acoustic emission rate was 100 events per minute. Over the next 63 minutes the acoustic emission rate dropped to 25 per minute. The emission rate then showed some sign of increasing for the next 3 minutes. It then increased in a monotonic manner for 5 minutes to a rate of 169 events per minute, at which point the specimen failed catastrophically. This experiment was repeated with essentially the same result observed. The implication from this experiment is that for this type of load condition the onset of failure could be detected some minutes in advance.

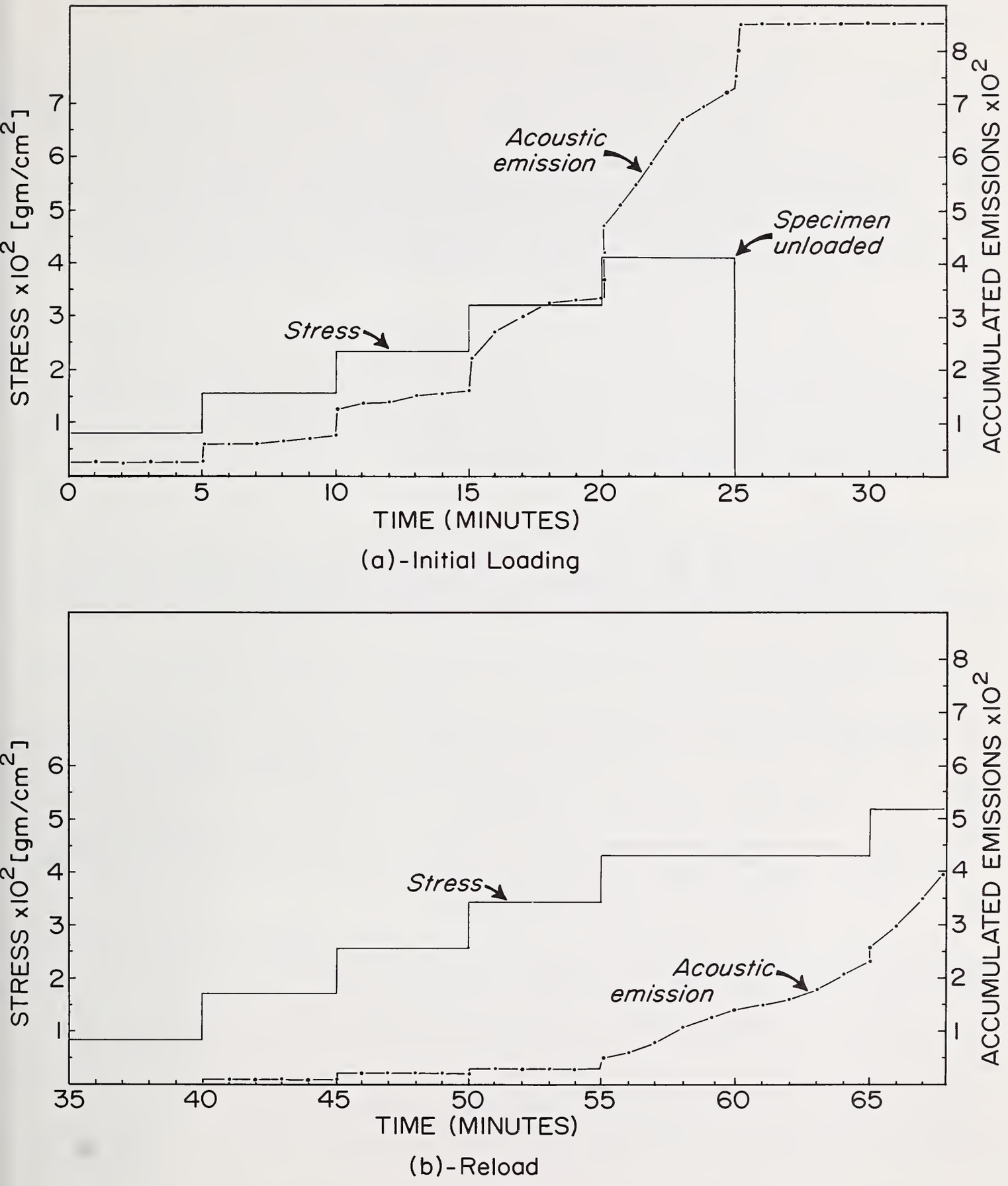

Figure 3. Accumulated acoustic emission response for a specimen subjected to an incremental load history: (a) Results of initial loading and unloading of snow sample; (b) Results obtained when specimen was reloaded.

Discussion

This paper has attempted to give a brief view of the acoustic emission phenomenon in snow. We have considered some possible emission sources and also presented the results of a number of laboratory experiments. In observing the acoustic emission phenomenon in snow, two possible applications in snow mechanics are suggested. As a purely empirical tool it appears that a great deal of information about stress and strain in an avalance slope may be gined by an acoustical monitoring system. Observations could be made both by placing transucers in an avalanche slope and making *in situ* observations and by removing samples and testing them in the laboratory. Using laboratory data as a basis, a comparative analysis could be made to interpret field data. One such test presently being investigated will utilize the Kaiser Effect to measure the state of stress over a period of time in a typical avalanche slope. If an oriented sample can be removed from the snowpacj without introducing spurious overstress in the process, it appears feasible that its *in situ* stress can be determined by controlled reloading in the laboratory.

A second possible research function of acoustic emissions would utilize this phenomenon, in conjunction with more standard techniques of experimental stress analysis, as an aid in the development of a constitutive relation for snow. At present the relation between acoustic emissions and the deformation mechanism in snow is not well understood. Consideration of the patterned acoustic response observed for various load and deformation histories indicates that it is related to the mechanical response. Since burst type emissions detected in snow originate from transient disturbances that take place in and between ice grains which compose the snow matrix, it appears reasonable to interpret the acoustic phenomenon at the structural level.

Acknowledgments

The authors wish to thank Dr. Glen L. Martin, Head, Department of Civil Engineering and Engineering Mechanics, Montana State University, for his support and interest in this work. We would also like to thank Dr. Theodore Land and Dr. Robert Brown for assistance with the research and for helpful criticisms of this paper.

This research is supported by Grant No. DA-ARO-D-31-124-71-G59 from the Army Research Office, Durham, North Carolina.

Literature Cited

Dunegan, H., and D. Harris.
1969. A new nondestructive testing tool. Ultrasonics 7(3):160-166.

Kinosita, A.
1967. Compression of snow at constant speed. In Physics of snow and ice, Hirobumi Ôura, Ed. Int. Conf. Low Temp. Sci. [Sappora, Japan, Aug. 1966] Proc., Vol. I, Part 2, p. 911-927. Inst. Low Temp. Sci., Hokkaido Univ.

Liptai, R. G., D. O. Harris, R. B. Engle, and G. A. Tatro.
1971. Acoustic emission techniques in material research. Int. J. Nondestructive Testing 3:215-275.

Sommerfeld, R. A., and E. LaChapelle.
1970. The classification of snow metamorphism. J. Glaciol. 9:3-17.

Tatro, C. A.
1971. Experimental considerations for acoustic emission testing. Mater. Res. Stand. II(3): 17-20.

Wakahama, G.
1967. Compression of a thin section of snow [motion picture]. In Physics of snow and ice, Hirobumi Ôura, Ed. Int. Conf. Low Temp. Sci. [Sappora, Japan, Aug. 1966] Proc., Vol. I, Part 2, p. 910. Inst. Low Temp. Sci., Hokkaido Univ.

INCORPORATION OF GLIDE AND CREEP MEASUREMENTS INTO SNOW SLAB MECHANICS

C. B. Brown, R. J. Evans, and D. McClung

ABSTRACT

The conventional field measurements in slab avalanche control include snow strength, creep, and glide. The snow strength appears naturally in any failure criterion, but the inclusion of creep and glide data into the slab mechanics is not obvious. Here, the physical features of creep and glide are discussed. This leads to possible models which can be incorporated into a continuum theory. As a result, definite suggestions are made concerning the range of parameters to be measured in the field.

Introduction

The solution of problems in snow slab mechanics can be based on the formulation of Perla and LaChapelle (1970) where some metamorphosis of either the snow ground interface or some surface in the snow slab causes a reduction in shear capacity. This approach has been further developed by Brown, Evans, and LaChapelle (1972) to find the state of stress in fallen snow and the dimensions of slab avalanches; this work provides no causality for the shear degeneration, and the boundary condition on the interface is described as zero normal motions and a definite shear stress. The solution used is linear elasticity theory.

The first shortcomings of the Brown, Evans, and LaChapelle work are: (1) The inability to model actual interface boundary conditions associated with definite metamorphosis; and (2) the inability to account for the nonlinear and temporal response of the snow. These two features are often included in the expressions, glide and creep. The object of this paper is to discuss the inclusion of these features into snow slab mechanics.

Glide

The relative motion between the ground surface and the juxtaposed snow will serve as a definition of glide. The motion is the measured translations over definite periods of time. It is natural to think of the onset of and subsequent motion being controlled by the laws of Amontons. These would mean that glide would not occur when

$$\tau < \sigma \mu_s \qquad [1]$$

where τ is the interface shear, σ the interface normal pressure, and μ_s the static coefficient of friction. When [1] becomes an equality, glide commences and the resistance to this motion is a shear

$$\tau = \sigma \mu_k \qquad [2]$$

where μ_k is kinetic coefficient of friction and $\mu_k < \mu_s$. One consequence of such laws is the monotonic increase of the glide speed with time. Examination of the results of Gand and Zupancic (1965) for glide near Davos indicates that the speed increases with time until a terminal value is attained. This speed is then maintained for the rest of the season. The results in figure 1 have a reverse trend inasmuch as the terminal speed is the decay from the high values of the earlier season. Clearly these two sets of readings from Davos and the Cascades are in conflict. However, they do refute the restraint equation [2]; the speed does stabilize in both cases, and the resistance must depend on the speed. Thus

$$\tau = f(v) \qquad [3]$$

where v is the glide speed. The functional form of [3] will apparently be completely different in the two cases discussed.

The small scale features at the interface consist of soft snow laid on a hard ground with the possibility of organic separation. The ground is rugged and, because of the differences between hardness of the ground and snow, it is unlikely that the usual concept of slipping can apply. Rowe (1964) has shown, for materials with very different hardness, failure is by shear in the softer material at a layer beyond the envelope of the rough surface. This means that failure

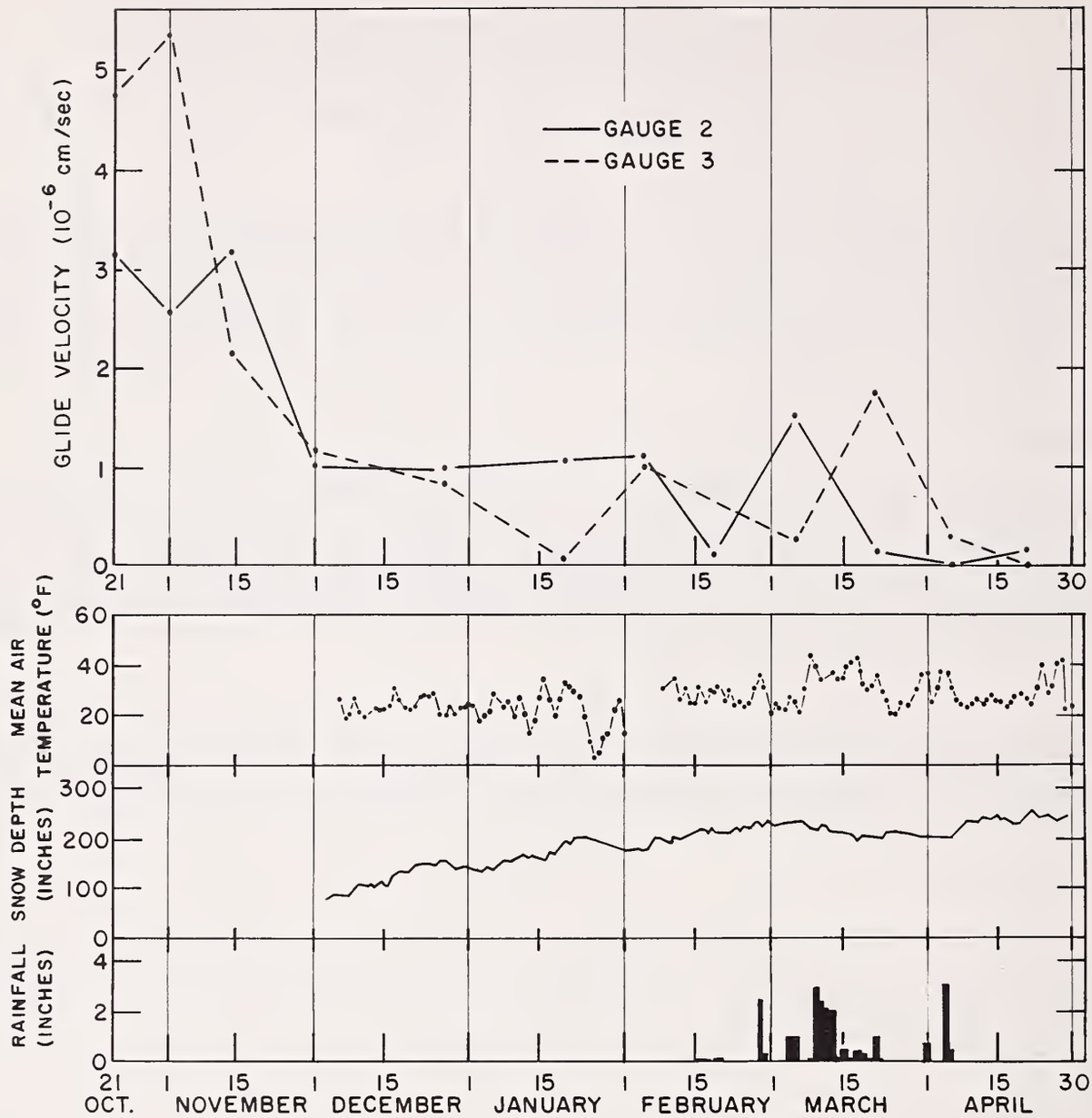

Figure 1. Glide measurements, 1971-72, Mt. Baker, Washington.

would be in the snow itself unless the organic layer was smooth and slippery or unless melt water appeared at the interface. Following up on Rowe's work, we would anticipate that the initiation of glide would be associated with the shear capacity of the snow. Here we would consider a sintered material with the conditions ripe for the application of the Bowden-Tabor (1958) theory of failure across the cohered interfaces of the grains. Unfortunately, in snow the phase state is dependent on the stress conditions as well as the temperature. The usual process of bond fracture at the interface occurs. This can be due to a combination of change of properties as well as the stress level. Healing may also happen. Thus, on the interface in the snow material a continuous process of healing and fracture, associated with regelation, must be expected.

The previous discussion suggests that once steady thermal and mechanical conditions exist near the interface, uniform glide speed should be attained. Until that steady state, the glide speed will depend on the presence of water, the organic layer, the snow condition, the slope and ground smoothness. Whether the glide accelerates to the terminal speed, as in the Davos work, or decelerates as in the work shown in figure 1, depends on these local conditions. The final steady speed will also be affected by the local conditions.

A conclusion concerning glide is therefore that a terminal steady speed will be attained once steady mechanical and thermal conditions exist. The prior speed will be closely associated with local characteristics.

A point with regard to the interpretation of field measurements of glide is worth noting. The glide velocity measured at a particular location depends not only on the interface conditions at that point but also on conditions at other locations on the moving interface, on the snow properties, and on the boundary conditions over the whole slope. Thus, meaningful comparison of results obtained at different sites and different geographic locations is particularly difficult.

Creep

This term is usually applied to deviatoric as well as dilational changes with time. The first is associated with the grains riding over each other, the second with grain readjustment toward a minimum bulk volume. Both processes are aided by the crystals tending to a spherical shape by loss of crystal branches due to vapor diffusion through the air spaces. The grain size decreases and the regime changes allowing local relocation and sliding to proceed rapidly. In spring time the process is aided by the intrusion of melt water from the surface. On a typical slope the creep occurs as motion parallel to and normal to the surface. Shear creep is manifested when the parallel velocity depends on the position of the snow. Dilational creep appears as settlement and uniform bulk motion down the slope. The strain rates in the two modes are of the same order of magnitude on avalanche slopes.

Figure 2 shows results of sawdust column tests in the Cascades. It is noted that the columns remain straight and that the shear creep strain rate is independent of position. This means that the shear strain is constant over the depth whereas the shear stress increases with depth; the constitutive law for the creep process of the snow is not that of a linear, homogeneous, isotropic material.

The creep speeds are of the same order as the measured glide speeds. Both features are therefore equally important in any analytical formulation.

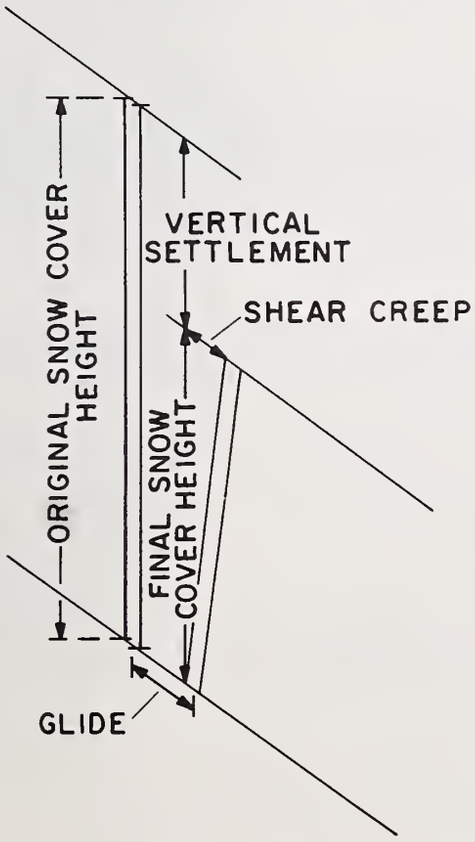

Figure 2. Typical creep experiment, Mt. Baker Site 3.

DURATION OF EXPERIMENT:
5.087×10^{6} sec (≈ 2 MONTHS)
SHEAR CREEP: 1.497×10^{-6} cm/sec
GLIDE: 0.2295×10^{-6} cm/sec
ORIGINAL HEIGHT: 422 cm
FINAL HEIGHT: 156 cm
SLOPE ANGLE: 30°, SOUTH-SOUTHWEST FACING SLOPE
TERRAIN: SHORT BRUSH AND GRASS

Glide Material

The glide boundary condition occurring with thermal and mechanical equlibrium appears to result in a uniform glide speed. At any time the total normal interface area, A, will be comprised of fluid and solid parts (A_F and A_S), thus

$$A = A_F + A_S \qquad [4]$$

The area A_F may in fact include separated interface regions discussed by Lang and Brown (1973). The only requirement is that A_F is unable to sustain shear stresses; then the apparent shear stress during glide is

$$\tau = \frac{\tau_s A_S}{A} \qquad [5]$$

where τ_s is the shear strength of the snow in the region A_F. This has a likeness to the Bowden-Tabor (1958) hypotheses. The area A_S will depend not only on the melting and freezing on the interface but also on the snow column weight. This affects the normal contact force on the sintered material considered here. An increase in normal force increases the contact area ($\bar{A}_S$) and results in a higher tangential force to cause incipient rigid body slip. Thus if N is the normal contact force, T the tangential force at the contact between two spheres at incipient slip, then

$$T = \mu_s N \qquad [6]$$

and

$$\tau_s = \frac{T}{\bar{A}_S} \qquad [7]$$

Because the increase in $\bar{A}_S$ with N is nonlinear, it is apparent that the value of τ in [5] is not only sensitive to the thermal state but also depends on the weight of the snow overburden. The importance of these aspects will vary from site to site.

A steady situation later in the season would be expected to produce an isothermal state, nonmodifying snow properties and fixed snow overburden. A possible relationship at this steady state between the interface apparent shear, τ, and the finite glide speed v is

$$\tau = B\, v^{-1} \qquad [8]$$

where v depends on A_S/A and B on the local conditions providing the values in [6] and [7].

Creep Model

Consideration of the material suggests that tractable problems in snow mechanics are generally of two types: (1) Those in which disturbances are of short duration and behavior is essentially elastic, and (2) those where loads are sustained for longer times and viscous flow is significant compared to initial elastic motions. For type (1) indications are that at least for low stresses a linear elastic law may be justifiable (Brown et al. 1972). For type (2), consideration of the material as either nonlinear or inhomogeneous lead to motions consistent with those observed. These two forms of steady creep law are investigated here.

For this purpose we will assume uniform slope and snow depth and constant snow density, ρ. Coordinates are as shown in figure 3 where an infinite extent in the x_2 plane exists. Then the known stress components, τ_{ij}, (Brown et al. 1972) are:

$$\tau_{12} = \rho \sin\Theta\, x_2 \qquad [9a]$$

$$\tau_{22} = -\rho \cos\Theta\, x_2 \qquad [9b]$$

$$\tau_{13} = \tau_{23} = 0 \qquad [9c]$$

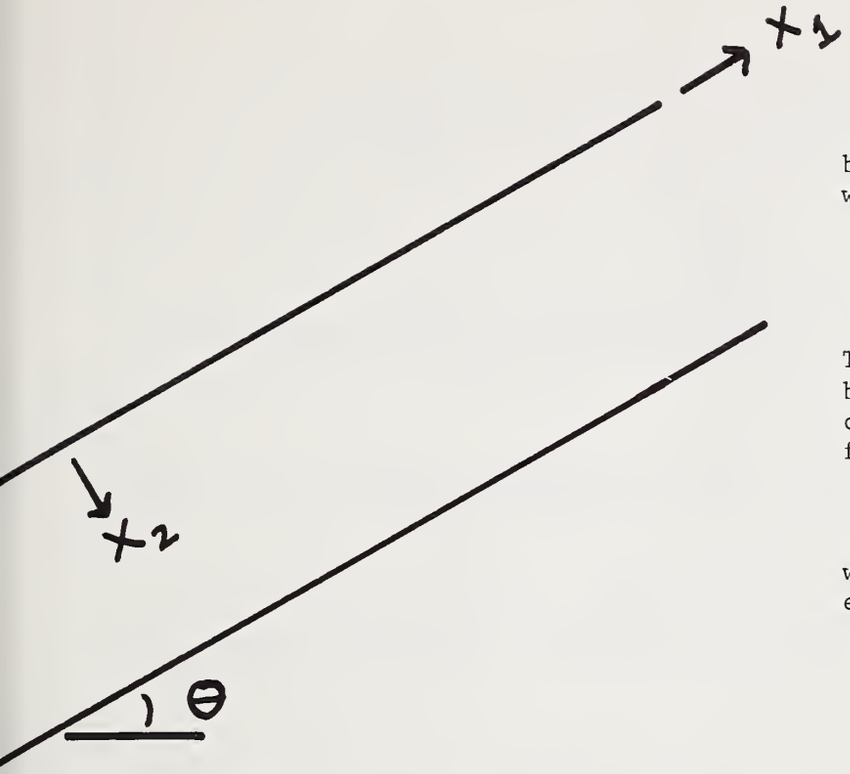

Figure 3. Coordinate system for creep model of long uniform slope.

Known strain rate components, d_{ij}, are:

$$d_{12} = k_1 \qquad [10a]$$

$$d_{11} = d_{33} = d_{13} = d_{23} = 0 \qquad [10b]$$

based on our experimental evidence (figure 2), we assume k_1 is constant.

Thus only d_{22}, τ_{11}, and τ_{22} are unknown.

(a) Nonlinear Isotropic Constitutive Law.-- To model an isotropic homogeneous relation between stress and strain rate for steady creep, we assume a constitutive law of the form (Salm 1967):

$$\tau_{ij} = F_1 \delta_{ij} + F_2 d_{ij} \qquad [11]$$

where F_1 and F_2 are functions of the independent strain rate invariants I_1 and I_2 and where

$$I_1 = d_{kk} \qquad [12]$$

$$I_2 = \frac{1}{2} d_{ij} d_{ij} \qquad [13]$$

From [10], for the state of deformation under consideration,

$$I_1 = d_{22} \qquad [14]$$

$$I_2 = d_{22}^2 + 2k_1^2 \qquad [15]$$

From [11]

$$\tau_{12} = F_2 k_1 \qquad [16]$$

which, using [9a] and [10a], give

$$F_2(d_{22}, d_{22}^2 + 2k_1^2) = \frac{\rho \sin\theta}{k_1} x_2 \qquad [17]$$

Clearly, the dependence of τ_{22} on x_2 must be known before proceeding further. This information is not presently available, however, and the general relation $\tau_{22}(x_2)$ will be assumed. It may readily be shown that [17] cannot be satisfied if d_{22} is constant. Assuming

$$d_{22} = k_2 x_2 \qquad [18]$$

where k_2 is constant, then [17] can be most simply satisfied if

$$F_2(I_1, I_2) = \alpha I_1 \qquad [19]$$

where α is a material constant.

Satisfaction of [9b] places restrictions on F_1 which using [11] become

$$-\rho \cos\theta \, x_2 = F_1 + \alpha (k_2 x_2)^2 \qquad [20]$$

[20] is most simply satisfied if

$$F_1(I_1, I_2) = \beta I_1 - \alpha I_1^2 \qquad [21]$$

and hence the simplest form of [11] consistent with observations is

$$\tau_{ij} = (\beta d_{kk} - \alpha d_{kk}^2)\delta_{ij} + \alpha d_{kk}\, d_{ij} \qquad [22]$$

and in terms of α and β the parameters of deformation, k_1 and k_2, are given by

$$k_1 = -\frac{\beta}{\alpha}\tan\Theta \qquad [23]$$

$$k_2 = -\frac{\rho \sin\Theta}{\beta} \qquad [24]$$

(b) Inhomogeneous Constitutive Law.--The observed shearing deformation will occur if

$$\tau_{12} = 2\Sigma d_{12} \qquad [25]$$

where Σ is a material constant which increases linearly with depth and is zero on the upper surface. Such inhomogeneity would result if the flow law for steady creep were of the form

$$\tau_{ij} = \lambda\delta_{ij} + 2\Sigma\, d_{ij} \qquad [26]$$

where λ and Σ are material constants which depend on invariants of the state of strain, that is, stress-induced inhomogeneity. The observed deformation would occur if Σ were linear in volumetric strain (or hydrostatic stress).

Argument (b) for inhomogeneous material provides a simpler explanation of the observed shearing motion than argument (a). For this reason, it must be preferred at this stage. Provided that λ and Σ are strain or stress dependent, then [26] still describes nonlinear material behavior. For some stages of creep, however, where the state of stress remains constant, the behavior will be equivalent to that of an inhomogeneous isotropic material. Clearly, further experimental evidence is required before more definite conclusions may be drawn with regard to the constitutive law for steady creep.

Avalanche Prediction

From the hypothesis of Perla and LaChapelle (1970) and the subsequent full analyses (Gand and Zupancic 1965), it is clear that one avenue of avalanche prediction concerns the attenuation of basal shear capacity. The regelation model suggested here for the steady speed case would mean that over a substantial total interface area A some part will be melted and some frozen. Additionally, separation may occur. Under these circumstances [4] and [5] apply. Over A_F the shear capacity will be zero whereas over A_S the capacity at incipient sliding will be τ_s. This will reduce when a value $\mu_k \leq \mu \leq \mu_s$ is introduced into [6]. Averaged over the interface, this will account for some regions slipping locally and some just on the point of slipping. A consequence is that as A_S/A decreases, the apparent shear capacity, τ, decreases and the glide speed increases. Thus the physical model for glide resistance of Gand and Zupancic (1965) and by figure 1 can be explained by the hypothesis of [5]. In this case, our interest is in the sense of the ration A_S/A and hence in the sign of the rate of change of glide speed with respect to time. When the glide speed is increasing, with no additional evidence of increase in snow strength, then conditions of incipient avalanching should be expected. With decreasing glide speed, the slope should be stabilizing. In figure 1 the increasing glide speeds in February forecast periods of danger because of the increase in A_F; the decreasing speeds in February and March give rise to confidence in the snow slope stability.

Acknowledgments

This work was sponsored by the Federal Highway Administration, U. S. Department of Transportation, and the Department of Highways, State of Washington. The opinions, findings and conclusions expressed are those of the authors and not necessarily those of the sponsors.

Literature Cited

Bowden, F. P., and D. Tabor.
1958. The friction and lubrication of solids. Oxford Univ. Press.

Brown, C. B., R. J. Evans, and E. R. LaChapelle.
1972. Slab avalanching and the state of stress in fallen snow. J. Geophys. Res. 77:4570-4580.

Gand, H. R., and M. Zupancic.
1965. Snow gliding and avalanches. Int. Symp. Sci. Aspects of Snow and Ice Avalanches, Davos, Switz., p. 230-242.

Lang, T. E., and R. L. Brown.
1973. On the mechanics of the hard slab avalanche. p. 24-28. In Advances in North American avalanche technology: 1972 symposium. USDA For. Serv. Gen. Tech. Rep. RM-3, 54 p. Rocky Mt. For. and Range Exp. Stn., Fort Collins, Colo.

Perla, R. I., and E. R. LaChapelle.
1970. A theory of snow slab failure. J. Geophys. Res. 75:7619-7627.

Rowe, G. W.
1964. Friction and metal-transfer of heavily-deformed sliders; mechanisms of solid friction. Elsevier Pub. Co., N.Y., p. 204-216.

Salm, B.
1967. An attempt to clarify triaxial creep mechanics of snow. In Physics of snow and ice, Hirobumi Ôura, Ed. Int. Conf. Low Temp. Sci. [Sappora, Japan, Aug. 1966] Proc., Vol. I, Part 2, p. 857-874. Inst. Low Temp. Sci., Hokkaido Univ.

MATERIAL PROPERTY AND BOUNDARY CONDITION EFFECTS ON STRESSES IN AVALANCHE SNOWPACKS

J. O. Curtis and F. W. Smith

ABSTRACT

A linear elastic finite element computer program was applied to determine the stress distributions in multilayered snowpacks typical of those found at Berthoud Pass, Colorado. The effect on stress distribution of wide variations in elastic material properties was examined. Also, an attempt was made to model the shear failure of a weak sublayer in the snowpack by relaxing the condition that the bottom snow layer be firmly attached to the ground.

Introduction

This paper discusses the progress made in a joint research effort between the Rocky Mountain Forest and Range Experiment Station and Colorado State University to develop a mathematical model for the prediction of stresses and displacements in an avalanche snowpack. In this work, the finite element method is being used to provide a flexible stress analysis tool which can easily accommodate the geometric complexities of a realistic snowpack. At present the finite element model only accounts for elastic effects and therefore ignores the realistic effects of creep and plasticity. In spite of this limitation a considerable amount of insight to the stress distribution may be gained by such analysis, and to this end the following work is presented.

A set of numerical experiments were conducted on the finite element model. The purpose of these experiments was to predict the variations in stress distribution which result from varying both the material properties of the snow and the boundary conditions along the bottom of the snowpack. This work is an extension of previous work by Smith (1972) in which the type of boundary condition along the bottom of the snowpack was very restrictive and in which the study of material property effects was incomplete.

In earlier studies the bottom layer of the snowpack was assumed to be firmly attached to the ground. To simulate a weak sublayer the modulus of elasticity of the bottom layer was taken to be an order of magnitude smaller than for the rest of the snowpack. An attempt has been made in the present work to refine the modeling of the weak sublayer condition by application of shear and normal stress perturbations to the bottom layer, an idea investigated by Perla and LaChapelle (1970). This is an attempt to model a condition in which a shear failure has occurred along the bottom of the snowpack.

There has been considerable interest in the orientation of the principal axes of stress, particularly in the region of the fracture line. This paper also presents information regarding the influence of varying material properties and boundary conditions on the principal stress directions.

Problem Statement and Analysis Technique

The analytical model was applied to a multilayered snowpack (fig. 1) found on Berthoud Pass, Colorado, U.S.A. Layer densities are labeled and the region of primary concern is shown. This snowpack was measured and observed during the winter of 1965-66 by members of the Rocky Mountain Forest and Range Experiment Station. A natural avalanche did take place on this location with the observed fracture line noted in figure 1.

The finite element computer program, utilizing triangular constant strain elements, was applied with the following assumptions:

1. Plain strain conditions exist in the snowpack.
2. The top surface is stress free.
3. Each layer is isotropic.
4. A constant value of Young's modulus and Poisson's ratio exists throughout the snowpack.

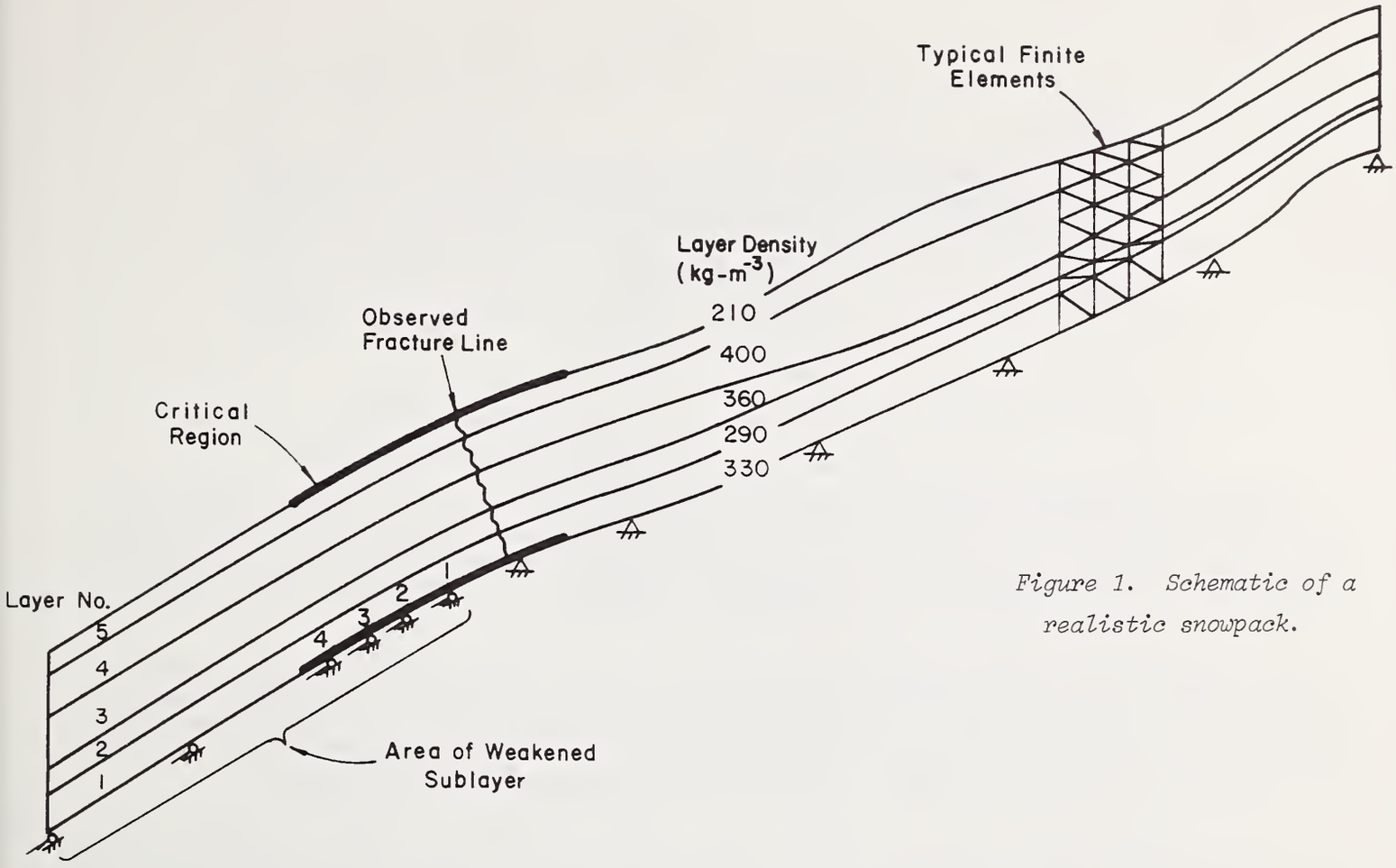

Figure 1. Schematic of a realistic snowpack.

A realistic snowpack such as the one shown in figure 1 is much longer than the figure indicates. In order to minimize possible errors due to truncating the snowpack, the approximate stress distribution due to Mellor (1968, p. 43-44) was applied to the left and right hand ends.

For part of the studies, a shear failure in a weak sublayer was assumed to exist over the area shown in figure 1, and was simulated by the following procedure. In the finite element method, as applied here, the snowpack is divided into triangular subregions with nodes at the vertices of each triangle. Once the numerical solution to a particular problem is complete, the stress and strain throughout each element as well as the net force and displacement at each node is known. To model the shear failure a computer run was first made in which the nodes along the bottom of the snowpack were assumed to be rigidly attached to the slope. This is called the "baseline" condition. The forces acting on the bottom nodes were then isolated for special study. The tangential components of these forces were reduced, and a new computer run was made to simulate a shear perturbation which might occur along the bottom of a snowpack due to the presence of a shear failure in a weak sublayer. For the present analysis, the forces were reduced in the following way (fig. 1): node point 1 had 100 percent of the baseline force applied to it; node point 2 had 90 percent, node point 3 had 80 percent, while node point 4 and the remaining bottom nodes had 70 percent of the "baseline" force applied.

This pattern of reduced forces is only one of many possible combinations which might be tried. The attempt here has been to determine whether this approach to modeling the weak sublayer has any validity at all in terms of the type of stress distribution produced compared to that expected based on field experience.

Results

Computer runs were made to predict the stress distribution within the snowpack for several combinations of values of the material properties (Young's modulus, E, and Poisson's ratio, ν). Analyses were performed for the "baseline" boundary conditions and for conditions for a shear failure in a weak sublayer. The following tabulation summarizes the cases which were run:

Young's Modulus $N-m^{-2}$	Baseline			Shear Failure in a Weak Sublayer		
	Poisson's Ratio			Poisson's Ratio		
	0.0	0.25	0.45	0.0	0.25	0.45
2×10^7	X	X	X	X	X	X
2×10^8		X				
2×10^9		X				

Effects of Material Properties.--Varying Young's modulus, E, had no effect on the stress distribution as long as the value of E was held constant throughout the snowpack. The reason for this is that the finite element method computes displacements as a function of the inverse of Young's modulus. Then stresses are computed as a function of E multiplied by the estimated displacements so that the effect of Young's modulus disappears.

The effect of Poisson's ratio on stresses in the snowpack is shown in figures 2 through 4. In these figures, the top graph presents the variation of the principal and maximum shear stresses with position along the top layer. The center diagram shows line segments which are alined with the direction of maximum principal stress. The lower graph presents the variation of the principal and maximum shear stresses with position along the bottom layer.

Two trends should be noted in these figures. First, values of principal stresses in the bottom layer become more compressive with increasing Poisson's ratio. The second trend to note is that there is a reorientation of the principal elements in the critical region of the snowpack. An examination of the principal element directions in the lower layer of snow shows that as Poisson's ratio increases, the principal directions rotate in a clockwise manner. The rotation is so great that for a Poisson's ratio of 0.45, the principal elements all lie at an angle of nearly 45° with respect to the slope of the layer below the observed fracture line. Remembering that the plane of maximum shear is oriented at an angle of 45° to the direction of maximum principal stress, it may be concluded that if a failure were to occur in the bottom layer of snow, it could occur as a shear failure. This result is interesting in light of a snowpack failure theory in which it is presumed that avalanche release initiates as a shear failure in a lower layer below the fracture line producing a tensile failure at the fracture line.

To carry this point further, one should compare the stress distribution resulting from the "baseline" runs with experimentally derived failure envelopes. Let us examine the maximum shear values found in lower layers below the observed fracture line for the $\nu = 0.45$ case.

Figure 8 shows that maximum shear stress value for layers 1 and 2 do lie within the shear failure envelope as constructed by Mellor (1966), while shear values for the other layers do not. Thus it is conceivable that shear failure could take place in either of these two layers. Field observations after the avalanche had released revealed that a shear failure did take place between layers 1 and 2.

One important difference between the shear stresses in these two layers is that the directions of maximum shear are different. Maximum shear in the bottom layer is oriented parallel to the hill's slope below the fracture line. This is not the case for layer 2. Therefore, one would expect that if a shear failure was to occur in the bottom layer, it would be in a direction parallel to the ground surface, while in layer 2 it would not.

It is also interesting to note that for all values of Poisson's ratio for "baseline" sums, the maximum principal stresses in the top layer tend to be tensile near the fracture line, but are not oriented parallel to the top surface. It might be reasonable to expect that the principal direction should be parallel to the top surface in order to produce a fracture plane upon failure which is perpendicular to the snowpack.

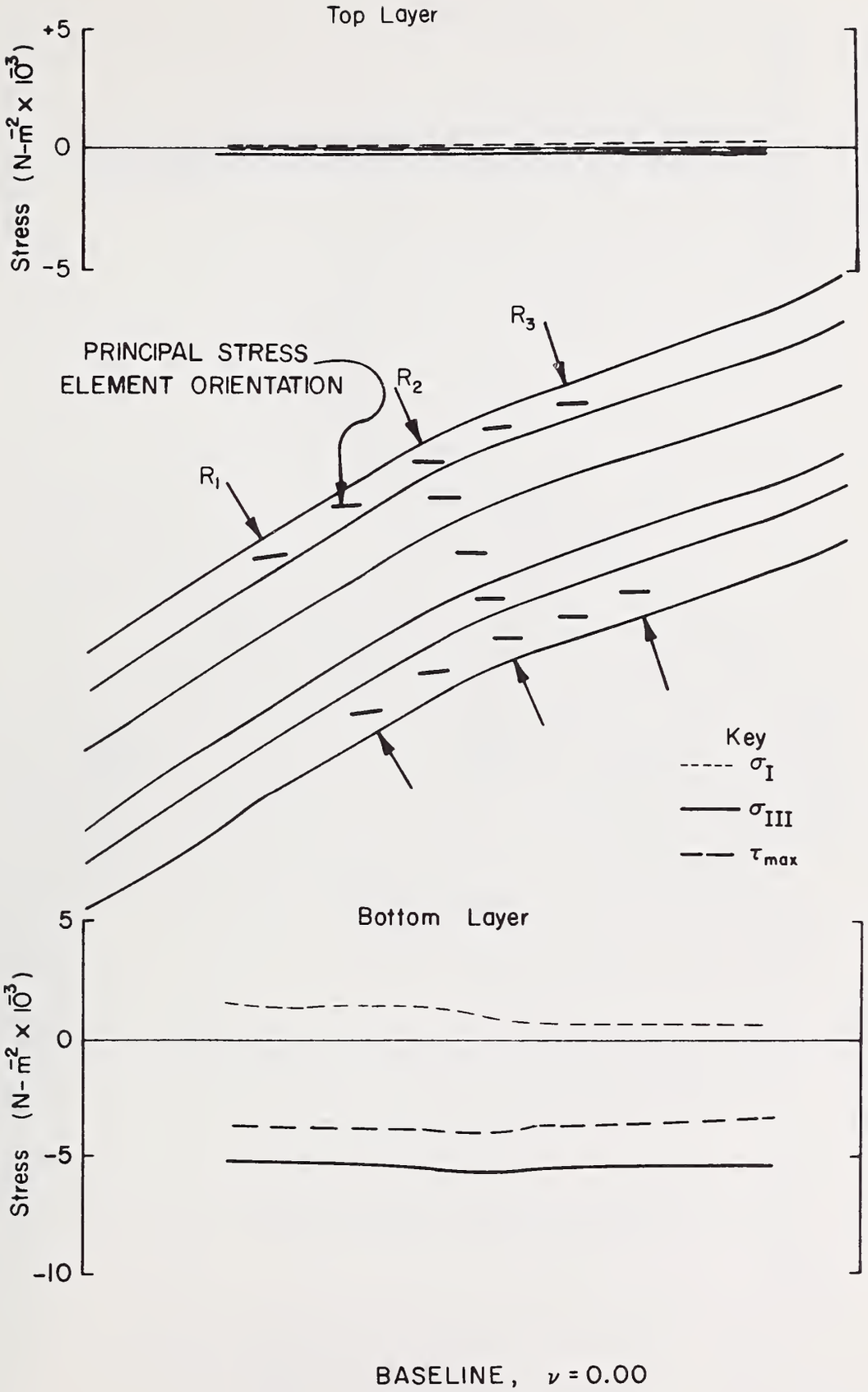

Figure 2. Principal stress magnitudes and directions.

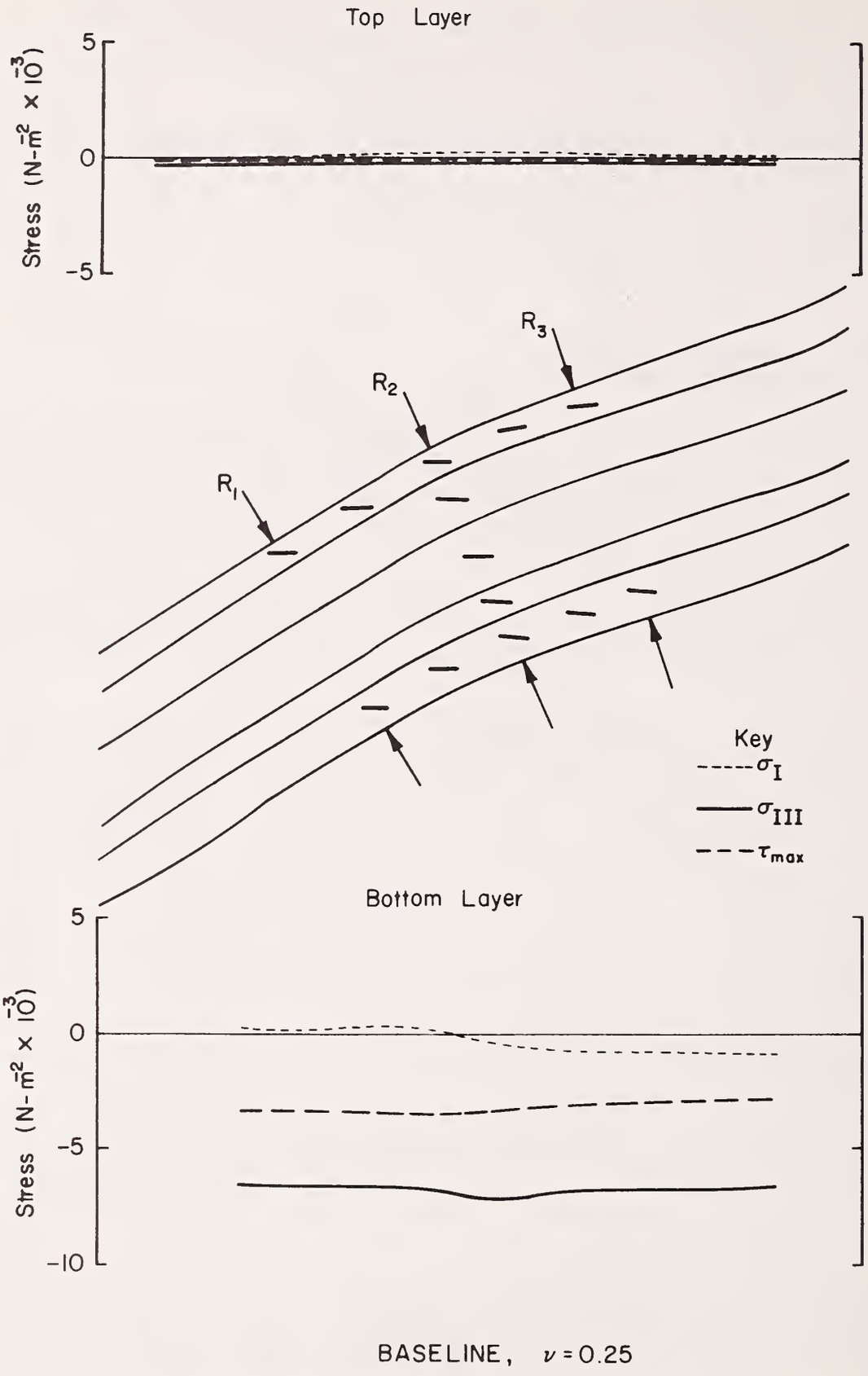

Figure 3. Principal stress magnitudes and directions.

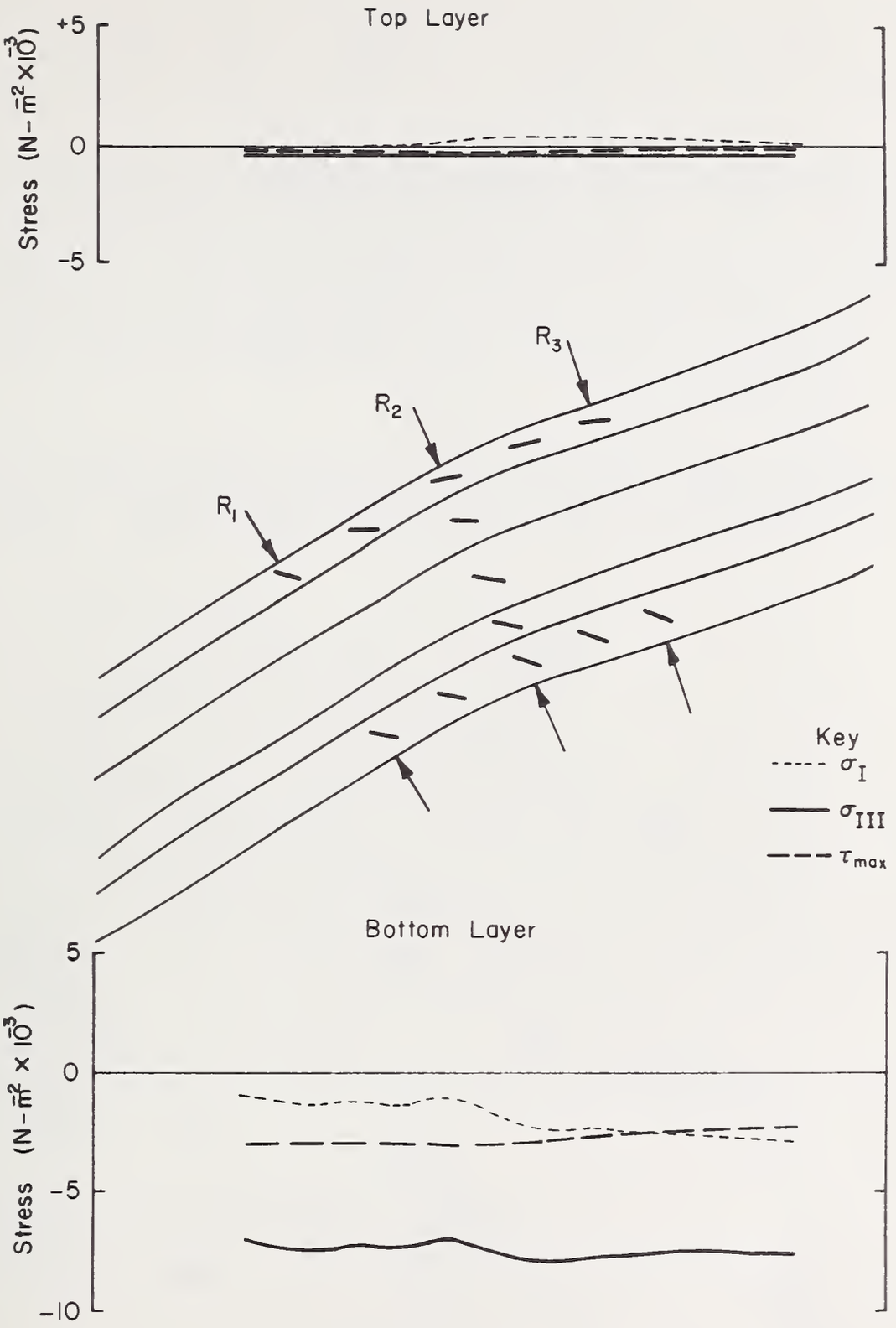

BASELINE, $\nu = 0.45$

Figure 4. Principal stress magnitudes and directions.

Figure 5 presents the "baseline" run for Poisson's ratio of 0.25 plotted in a different way to illustrate the variation of stress through the snowpack in a direction perpendicular to the snow surface. A stepwise linear variation in the stresses is noted. This is due to the fact that the stresses are heavily controlled by the snow density. Since the density of each layer is different, the slope of the stress variation in that layer is expected to be different.

Effects of a Shear Failure in a Weak Sublayer.--Figures 6 and 7 graphically display the results of reducing tangential loads at the base of the snowpack to model the shear failure. There are two primary effects to be noted. The first and most obvious effect produced by the weakening of the sublayer is to create a stress concentration just below the observed fracture line. Comparison of figures 3 and 6 for a typical value of Poisson's ratio clearly demonstrates how the stresses change in the snowpack as a result of weakening the bottom layer. Along the top layer, the state of stress changes from one of near zero stress to one in which the maximum principal stress is fairly large and tensile. One also finds that the principal element in the reduced load case is directed parallel to the top surface. Both observations tend to support the theory of avalanche release that points to a shear failure in the snowpack followed by a tensile failure near the surface as the release mechanism.

Changing Poisson's ratio affected the reduced load stress distribution in nearly the same way that it did for baseline runs. Without referring to additional figures, the analysis showed that increasing Poisson's ratio had little effect on principal stress magnitudes for the shear failure calculations, but that there was a reorientation of the principal elements. Increasing Poisson's

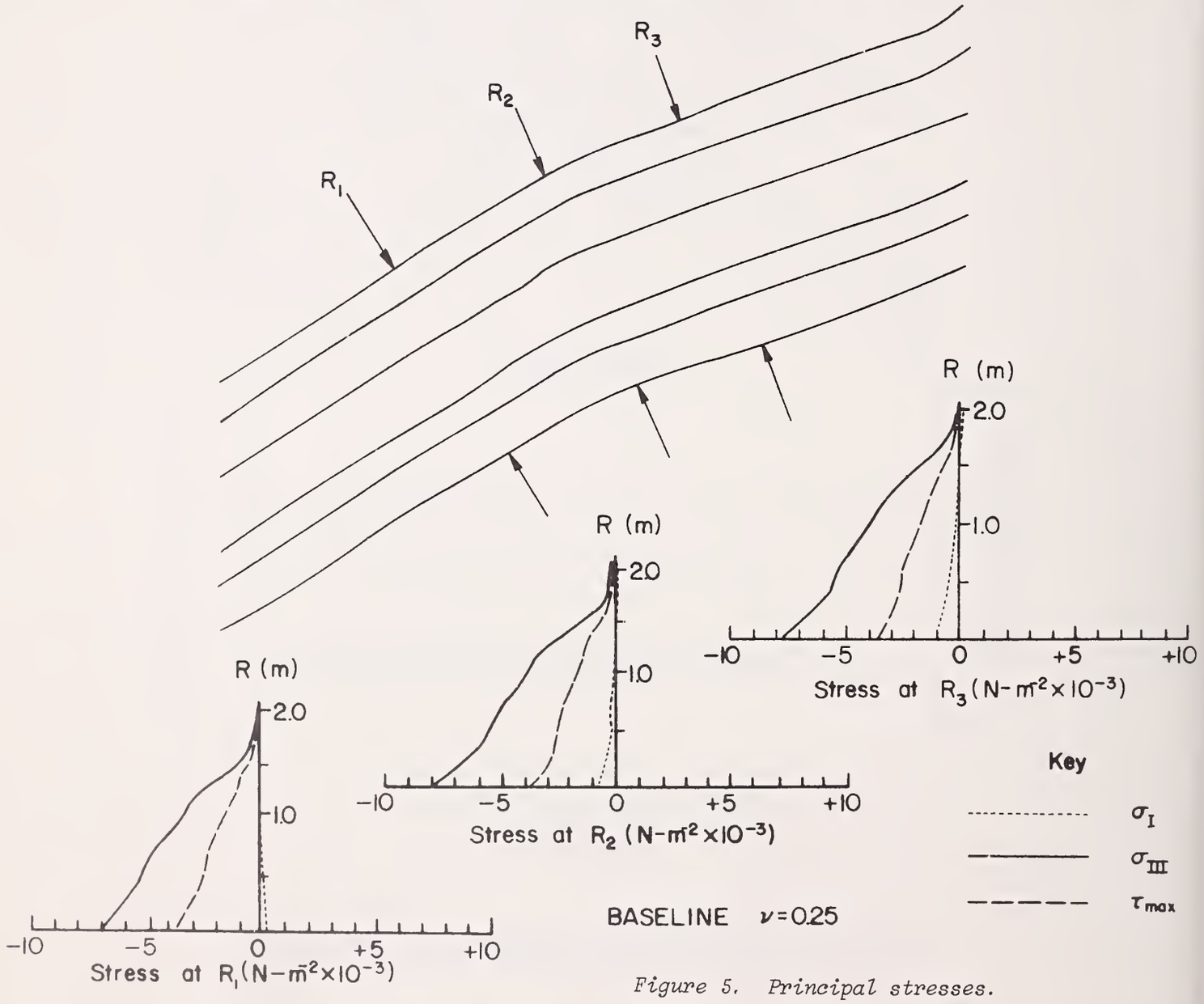

Figure 5. Principal stresses.

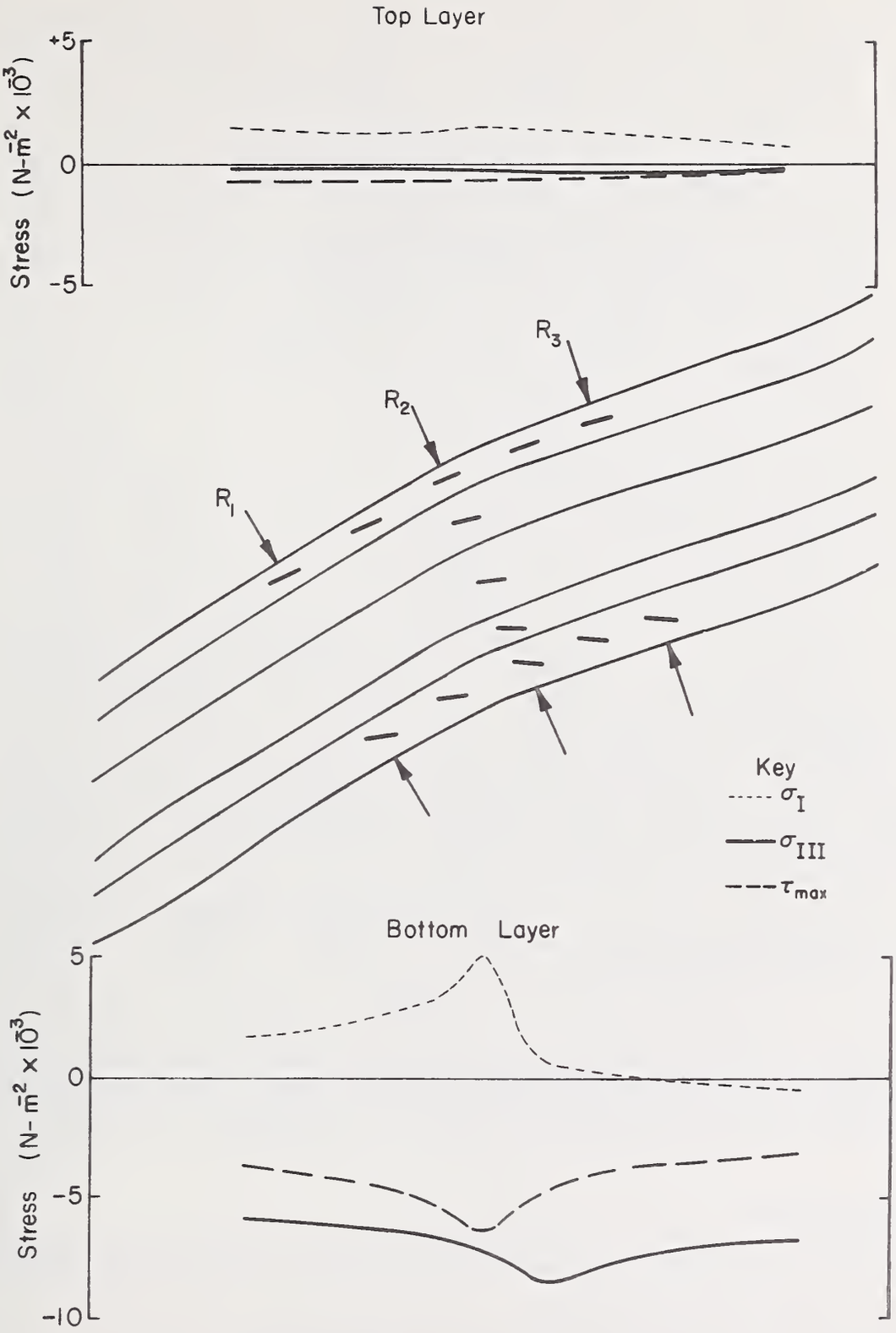

Figure 6. Principal stress magnitudes and directions.

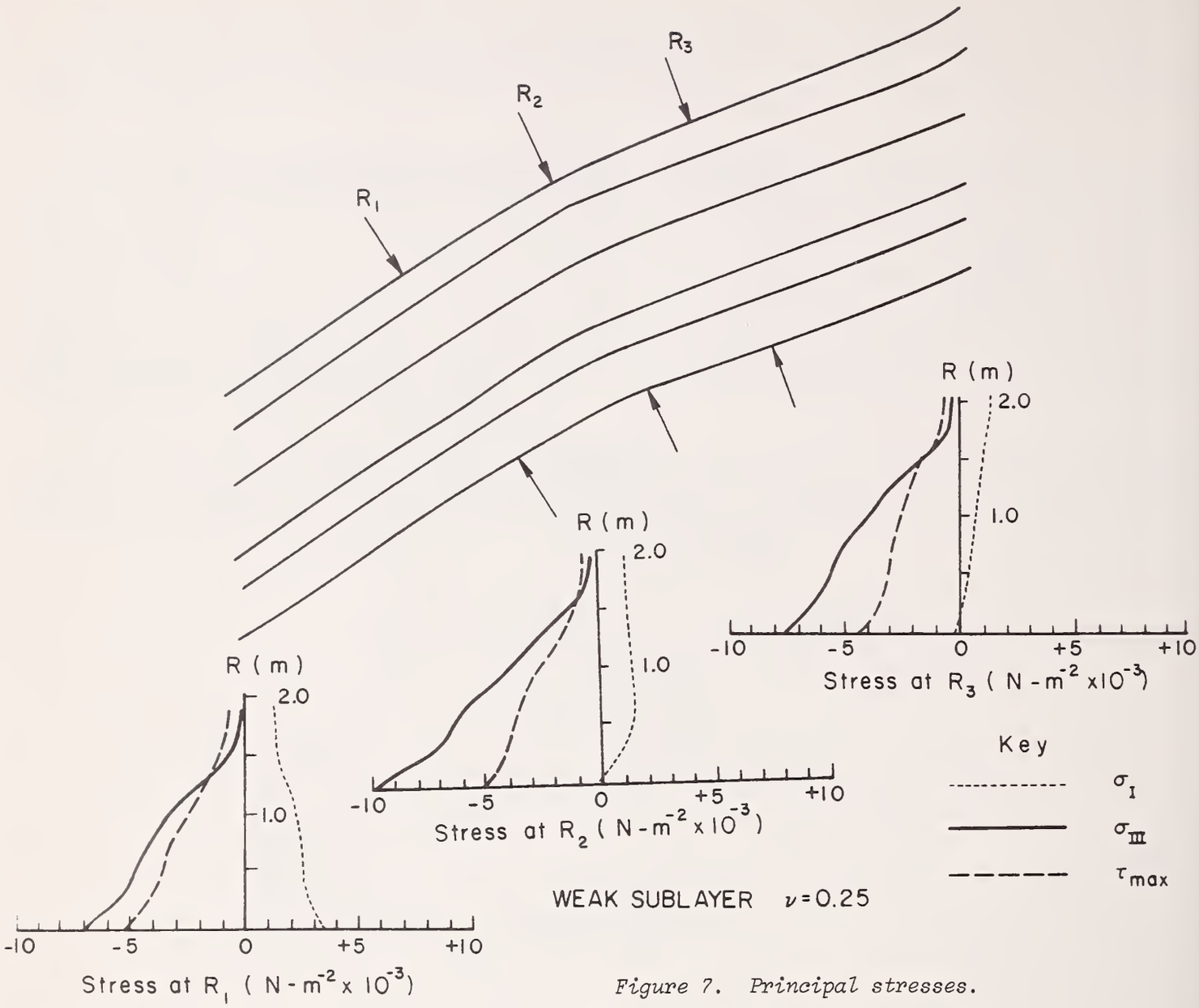

Figure 7. Principal stresses.

ratio caused a small clockwise rotation of the principal elements in the bottom layer, but had no effect on principal stress directions in the top layer. It should be made clear, however, that the state of stress in the lower layer was no longer one of maximum shear oriented parallel to the slope, since the shear failure simulation resulted in a redistribution of stresses.

Summary and Conclusions

Conclusions that can be drawn with respect to the effect of varying material properties are:

1. Varying a uniform Young's modulus does not influence the stress distribution in the snowpack.
2. Increasing Poisson's ratio makes the principal stress values more compressive, while for the most part rotating the principal elements in a clockwise direction.
3. Layers of variable density snow influence the variation of stresses as a function of depth. Density will play an even greater part when Young's modulus and Poisson's ratio are made functions of this parameter.

The above analysis was not an attempt to verify any particular avalanche failure theory; however, two conclusions can be drawn that tend to substantiate field observations of this and other avalanche snowpacks. First, the baseline runs revealed that a shear failure could have taken place in the bottom layer of snow below the observed fracture line. Post-release investigations of the actual snowpack revealed that such a failure did take place. Another important result of the

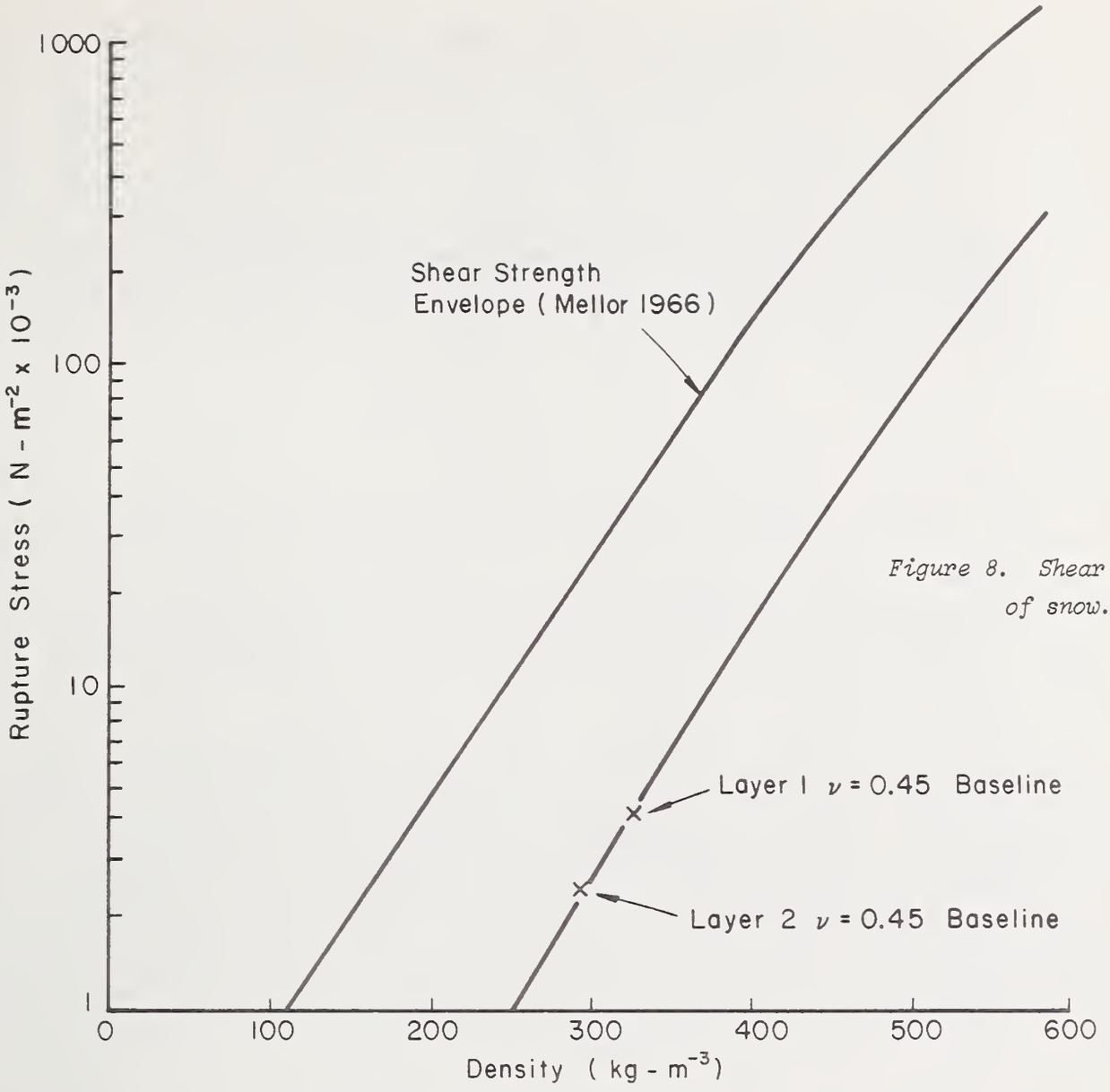

Figure 8. Shear strength of snow.

analysis is that through shear failure simulation, large tensile stresses parallel to the snow surface can be generated within the top layer of snow. This condition might lead to tensile failure in the critical region. Once again, field observation verified such an occurrence.

Acknowledgments

The authors are grateful to Drs. R. A. Sommerfeld and R. I. Perla of the Rocky Mountain Forest and Range Experiment Station, Fort Collins, Colorado, U.S.A. for their many helpful suggestions in the course of this work.

Literature Cited

Mellor, M.
1966. Snow mechanics. Appl. Mech. Rev. 19(5): 379-389.
Mellor, M.
1968. Avalanches. Cold Regions Science and Engineering. Part III: Eng., Sect. A3: Snow Technology. U.S. Army Materiel Command, Cold Regions Res. and Eng. Lab., 215 p. Hanover, N.H.
Perla, R. I., and E. R. LaChapelle.
1970. A theory of snow slab failure. J. Geophys. Res. 75:7619-7627.
Smith, F. W.
1972. Elastic stresses in layered snowpacks. J. Glaciol. 11: 407-414.

ON THE MECHANICS OF THE HARD SLAB AVALANCHE

T. E. Lang and R. L. Brown

ABSTRACT

The buckling of snow slabs is proposed as a failure mechanism of avalanche slopes. Preliminary results indicate that buckling may initiate and grow under a wide range of conditions. To study the problem further, nonlinear constitutive equations and nonlinear failure theories are being considered. Acoustic emission techniques will be used to characterize the behavior of snow.

Introduction

Various factors contribute to the recognized uncertainty over the mechanism of hard slab snow avalanche release. Perhaps the greatest difficulty is the hazard of field observation of other than the crown region of an avalanche-sensitive slope. Additionally, downslope preavalanche material and conditions of geometry are largely obliterated following the avalanche. The upslope or crown region postavalanche geometry remains intact, and has been monitored and studied in some detail. Theories of release have been formulated assuming initial disturbance in the crown region, as by a tensile stress fracture, and subsequent propagation downslope (Sommerfeld 1969).

Snow, not being an easy material to characterize rheologically, has complex load-deformation properties and exhibits unique structure changes under certain thermal history conditions. In general, load, deformation, microstructure, and thermal characteristics of snow *in situ* on slopes have not been systematically measured, so that quantitization of factors relevant to subsurface conditions are not known. However, recognizing the fact that physical changes occur in the interior of snowpack, release theories have been formulated based upon some type of basal layer inhomogeneity. It is assumed that material transformation or a form of inclusion produces a weakened state or an unstable structural configuration. Either from local collapse or a shear failure, the release ensues (Bradley and Bowles 1970, Haefeli 1966, Roch 1966). Recent work which supports this concept of a weak sublayer are the theoretical studies of the stress state associated with this geometry (Perla 1971, Brown et al. 1972a), and an order-of-magnitude evaluation of the feasibility of a buckling mechanism contributing to the enhancement of slope failure (Lang et al. 1973). These studies relate to subsurface and toe region influence upon the release question.

If, indeed, these mechanisms exist and affect release, then experimental and modeling techniques will have to be developed to aid in evaluating their importance. Based upon evidence now known, it is reasonable to assume the existence of a weakened basal layer condition. But there may be a number of disturbance types or imperfections which induce the triggering of the avalanche as the slope, by some process or other, reaches a critical stability state. If monitoring and control of the avalanche sensitivity of a slope is desired, then the important question is what physical changes occur early enough and with sufficient magnitude to reliably serve as a measure of slope stability. One possible macroscopic mechanism that may be detectable is local buckling of the slope. Evidence of long term large-amplitude buckling of snowpack is well documented, and the question arises whether buckling is a primary or secondary mechanism in avalanche release. Lacking conclusive experimental evidence of the importance of buckling, the concept is further explored in the remainder of this paper.

Material Representation for Buckling Analysis

The formulation of a possible buckling state is strongly dependent upon an adequate material characterization. To date an extensive variation exists in the constitutive properties used to study snow response. Most analyses are based upon linear constitutive equations, and time dependence expressed by a deformation or strain rate term (viscous response). In setting up a buckling model, it would appear that refinement in the constitutive law to account for more than one rate dependence can be treated. In constitutive law modeling to date, a linear viscoelastic model of low density snow has been reported by Shinojima (1967); however, in the absence of stress relaxation considerations, the model is based upon long-term fluid behavior. Results by Yosida (1966)

and in tests conducted by the authors (Brown et al. 1972b), long-term solid material residual is observed, in that complete stress relaxation under constant deformation does not occur. An additional complication report by Shinojima (1967) is that the linear form of the constitutive equations is different for each type of loading investigated, which included simple tension, compression, and torsion. Thus, different material coefficients should be used depending upon local stress conditions. However, this form of material nonlinearity should not be a primary factor in formulating a buckling criterion. The existence of a weakened sublayer, which is generally recognized as a necessary condition for slope instability, results in incomplete stress transfer to the slope bed surface and a transmittal and intensification of bearing stress downslope. Thus, the toe region material is in a state of compression, which simplifies the requirements on the constitutive representation.

The nonlinearity noted by Shinojima (1967) in transition from a compression to a tension state is reflected also in his reported values of Poisson's ratio. In tension the Poissonic effect approaches that of an equivoluminal material, whereas in compression the Poissonic effect is small. This difference in material behavior under different types of loading is attributable to the skeleton crystal structure of snow, in which both volumetric and distortional deformation mechanisms act. This is markedly different from typical viscoelastic modeling assumptions, but should be accounted for in setting up a viscoelastic model of snow.

What is perhaps the greatest impediment to a simple constitutive representation of snow is the fact that snow behaves strongly nonlinearily to changes in deformation rates, loading sequences, etc. Yosida (1966) indicates a strong nonlinear relationship between normal stress and low strain rates in simple compression tests of snow columns. Application to analysis of buckling can be handled by equivalent linearization of the constitutive model in the standard method of treating material nonlinearity.

The behavior of snow is complicated by its dependence on a number of items, which includes temperature, density, and state of metamorphism. The state of metamorphism, as indicated by Yosida (1966) can be characterized in terms of the thermal history and stress history of the material. These considerations therefore make the complete thermomechanical characterization of snow an extremely difficult task to undertake. However, this approach of characterizing snow is probably not necessary for making a comprehensive analysis of the problem of buckle mode growth. It is quite possible, as indicated by Yosida (1966), that a large portion of the snow slab may be metamorphically stabilized during the months of January through March, and that the timewise variation of the material properties may be negligible. If this is the case, the material aging characteristics and thermal history effects may be neglected in formulating the material constitutive equations, which must necessarily be nonlinear. However, since the stress distribution in the downslope region of an imperfection zone in the slab is compressive, the use of equivalent linear constitutive equations can be considered a valid simplication. However, more research needs to be done to verify if this can be done. Some questions pertaining to this which must be answered are: first, the extent to which one simplified constitutive equation can be utilized to represent the entire slab (that is, the effect of density variation and the percentage of the slab which does stabilize metamorphically), and, second, the correlation between stabilization of metamorphosis and macroscopic material properties.

In summary, the key to the analytic treatment of the buckling question is a refined model of the constitutive representation coupled with simplifying assumptions on the range of parameters based upon the physical conditions of the slab buckling phenomonen.

Physical Characteristics of Snow Slab Buckling

Two buckling geometries can occur. One is buckling of the surface layer of the snowpack while supported by a bed surface cushion. This requires either an interstitial weak layer (as from water percolation or material stratification), or a metamorphized basal layer (as from formation of depth hoar). Perla (1971) determined from examination of a number of postavalanche slopes that in 65 percent of the cases depth hoar was in evidence. Admitting the mechanism of long-term buckling, the wave shape of a typical buckling mode induces local regions of bearing stress intensification on the basal layer of depth hoar. This overstress enhances the brittle fracture and collapse of the depth hoar matrix, and, thus, is a plausible mechanism as an initial triggering source.

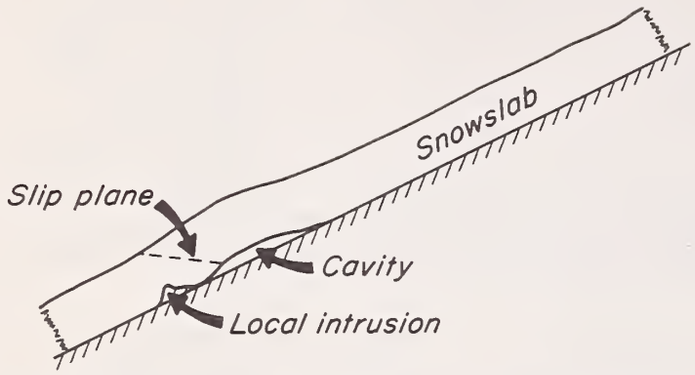

Figure 1. Geometric and stress intensification configuration due to local slab buckling.

Figure 2. Rise time versus relative overburden length for specified initial imperfection amplitude to wave length ratio of 0.05.

The second buckling geometry is the formation of a buckling pattern of the entire slab, which implies cavity formation at the bed surface. Two alternatives exist here, that either the cavity exists and buckling follows, or that the tendency for buckling produces the cavity. Whichever is the case, the formation of a buckle lobe in the toe region produces a geometric and stress intensification configuration that enhances the formation of a slip plane (fig. 1). Alternately, the feasibility of a buckling mechanism "locking" a slope must also be examined.

To examine the question of whether or not buckle formation is physically possible in snow slabs, (1) snow columns were tested in compression, and (2) the material coefficients determined were used in a buckling analysis. Snow columns of nominal length 20 cm, and specific weight 0.39 gm/cm^3 were tested at -10° C at constant deformation rates up to 0.005 cm/min. The load-deformation data were fit by a linear three-element viscoelastic solid model, and a buckling analysis procedure was followed (Lang et al. 1973). Results of the computations are shown in figure 2. The interpretation is that for a given length of bed-surface imperfection having an initial amplitude 0.05 of its length, the curve shown is the boundary between growth and subsidence of the imperfection. The abscissa is the factor indicating the number of equivalent lengths of imperfection that must be bearing onto the imperfection zone to yield a corresponding rise time for an order-of-magnitude change in the amplitude of the imperfection. Thus, for an imperfection of length, ℓ, snow of equivalent length 4ℓ must bear onto the imperfection zone in order that the amplitude of imperfection increase by a factor of ten in 10^3 hrs or approximately 41 days. Thus, even though the snow specific weight is high and the test temperature is low for midalpine snowpack (both factors, if adjusted accordingly, decrease the time for amplitude growth), a reasonable estimate of a buckling mechanism is obtained.

To further define whether or not subsurface imperfections can form, a snow slope in the Bridger mountain range north of Bozeman, Montana, having a history of avalanche activity, was selected. A 40-meter-long trench was dug along the nominal 40° slope approximately one-third of the distance in from the left flank of the snowpack, which terminates into tree and rock outcrops on both flanks and at the crown. Void imperfections were found (fig. 3), which encompassed 40 percent of the 40-meter length. All voids were easily distinguishable, the largest having an amplitude of approximately 12 cm, and all voids extended under the snowpack indicating the exposed section probably was typical. Approximately 5 meters from the crown region tree outcrop a crack 20 meters in length and 0.3 meter in maximum separation ran parallel to the outcrop. The existence of this crack indicates that the particular slope was in a state of glide. However, the significant fact is that the void formation mechanism was more pronounced than snowpack settlement, which would cause subsidence of the voids. Thus, it is probable that slope creep rate relative to snowpack settlement rate is an important parameter on whether voids form or not. Once voids develop, any weakened subsurface condition that would result in incomplete shear stress transfer to the bed surface would reinforce void growth.

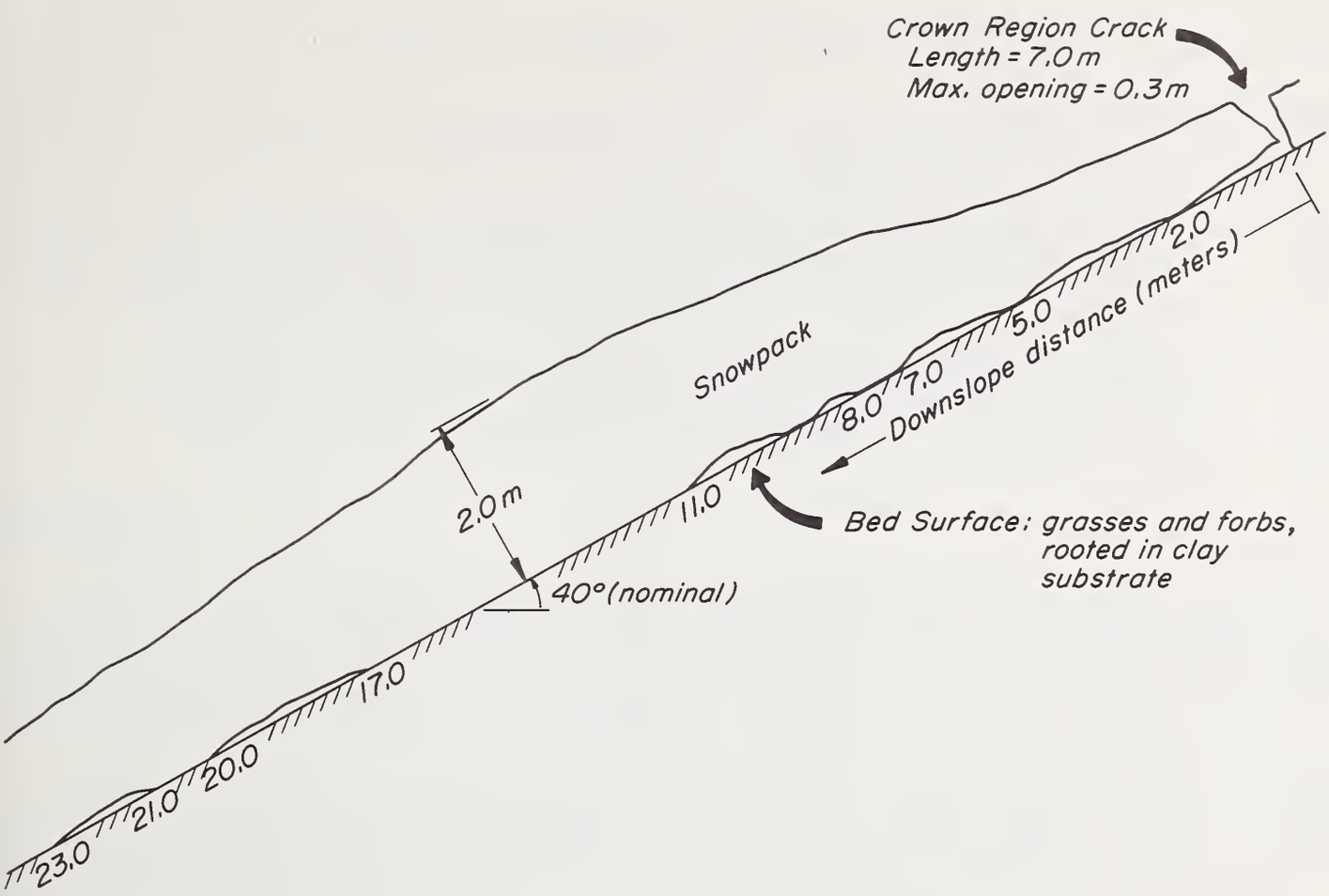

Figure 3. Slope cross section showing base lift-off, Bridger Range, Montana, January 19, 1972.

Final consideration is here given to a geometric profile described by Perla (1971). He indicates that the flank fracture profile of an avalanche zone has the shape of a sawtooth in a majority of cases. The sawtooth slants downslope, and conforms exactly to what would be predicted if a buckle wave with a downslope sagging central region were present immediately preceding avalanche release. Although the flank regions are influenced strongly by edge intrusions of rocks, trees, etc., if regular dimensions can be ascribed to the sawtooth pattern, this might relate directly to dominant buckling mode dimensions. Perla reports no data of this type, and the authors find none available in the literature.

Conclusion

Based upon the initial evidence concerning slab buckling, it appears that the possibility of a buckling state developing in avalanche-sensitive slopes must be considered. Using a simplified analytical model and nominal material properties, the times computed for buckle mode growth are at least of the same order as times associated with the avalanche phenomenon. The possibility exists for void formation and growth, depending upon the relative rates of snowpack settlement and slope-parallel creep, coupled with the necessity of a structurally weakened basal-plane zone. Also, evidence may exist on the flank region fracture profile that may correlate with dominant mode buckling pending further study and data acquisition.

Since buckling is a structural phenomenon extending into the toe region of the slope, physical measurement of void formation and buckle mode growth is difficult. Evidence of buckling from surface measurements is probably inconclusive because of wind transport of material that would obliterate long-term geometry changes. Thus, advanced *in situ* techniques such as acoustic emission monitoring, or slope modeling techniques, may be required to further assess the toe region influence on avalanche release.

Literature Cited

Bradley, C. C., and D. Bowles.
1970. The role of stress concentration in slab avalanche release: Comments on Dr. R. A. Sommerfeld's paper. J. Glaciol. 9:411.

Brown, C. B., R. J. Evans, and E. R. LaChapelle.
1972a. Slab avalanching and the state of stress in fallen snow. J. Geophys. Res. 77:4570-4580.

Brown, R. L., T. E. Lang, W. F. St. Lawrence, and C. C. Bradley.
1972b. A failure theory for snow. Presented at 3d Int. Discuss. Conf. [Prague, Czech., Sept.] on Gen. Princ. Rheol.

Haefeli, R.
1966. Stress transformation, tensile strengths and rupture processes of the snow cover. p. 141, In Ice and Snow, MIT Press, Cambridge, Mass.

Lang, T. E., R. L. Brown, W. F. St. Lawrence, and C. C. Bradley.
1973. Buckling characteristics of a sloping slab. J. Geophys. Res. 78:339-351.

Perla, R. I.
1971. The slab avalanche. U.S. Dep. Agric., For. Serv., Alta Avalanche Study Center, Alta, Utah, Rep. 100, 99 p.

Roch, A.
1966. Les declenchements d'avalanches. Int. Symp. Sci. Aspects of Snow and Ice Avalanches, Gentbrugge, Belgium, Int. Assoc. Sci. Hydrol., Pub. 69, p. 182-195.

Shinojima, K.
1967. Study on the viscoelastic deformation of deposited snow. In Physics of snow and ice, Hirobumi Ôura, Ed. Int. Conf. Low Temp. Sci. [Sappora, Japan, Aug. 1966] Proc., Vol. I, Part 2, p. 875-907. Inst. Low Temp. Sci., Hokkaido Univ.

Sommerfeld, R. A.
1969. The role of stress concentration in slab avalanche release. J. Glaciol. 8:451-462.

Yosida, Z.
1966. Physical properties of snow. p. 485, In Ice and Snow, MIT Press, Cambridge, Mass.

STATISTICAL PROBLEMS IN SNOW MECHANICS

R. A. Sommerfeld

ABSTRACT

Different types of statistical treatments are appropriate for evaluating measurements of different physical properties of snow. For density measurements, the mean and standard deviation of the measurements are meaningful parameters. In the case of strength measurements, the mean is not a very useful parameter, and some type of extreme-value statistics should be used. Weibull statistics appear to be appropriate for tensile strength data, while the thread bundle statistics of Daniels appear appropriate for the evaluation of shear strength data.

Introduction

Snow is a variable material; since most of its variations are random, statistical methods are indispensable in evaluating its behavior. Until recently, the statistical techniques applied to snow have been fairly simple. They have largely consisted of the calculation of the mean and sometimes of the standard deviation or confidence intervals of a series of measurements. Generally the measurements show such large scatter that attempts to correlate the various properties of snow have been frustrated.

Statistical techniques are available which can aid in a much better understanding of the behavior of snow and the relationships among its properties. It is necessary to use different kinds of statistical presentations, however, to extract the needed information from a series of experimental measurements. The appropriateness of a particular statistical technique depends on the properties being measured and the information desired from the measurements. As examples, we will examine statistical techniques which may be applied to density, brittle tensile strength, and shear strength data. Since the presence of free water in snow adds complications, this discussion will be limited to dry snow, although most of the concepts can be applied to wet snow as well.

None of the arguments presented are intended to be exhaustive. They are, rather, first attempts in this field; if they find application it will certainly be with extensive additions and modifications.

Snow Density

Dry snow is an intricate network of interconnecting ice crystals surrounded by air. The physical properties of ice and air are very different, and the volume ratio of ice to air can vary by over an order of magnitude. It seems obvious that the physical properties of snow must be related in very basic ways to the relative volumes of ice and air in a sample. The easiest measure of relative volumes is the density of the snow sample.

The variability of snow density is highest on a microscopic scale. If we were to proceed through a volume of snow taking 0.1 mm^3 samples at random, we would find some samples that were pure ice and some that were pure air. The data would range over values different by a factor of 10^3, but their mean value would be a measure of the bulk density of the total volume under consideration. Later we will see that this simple relationship between large and small samples does not hold for all of the properties of snow.

If consideration is restricted to density variations within major layers, the minor layering can be treated as statistical variations within the major layers. A careful study of the coefficients of variation within various sample volumes would answer the question of whether or not the densities of the major layers in an avalanche starting zone can be adequately determined from samples taken in a smaller volume. No study has been carried out with this approach in mind, but some data are available from other studies.

Martinelli (1971) measured the densities of 84 pairs of samples, each pair taken within a major layer. Each pair of $0.5 \times 10^{-3} m^3$ samples was taken in close proximity so that the

variability between the members of each pair is a measure of the variability within sample volumes of about 2 x $10^{-3}m^3$. The mean coefficient of variation between the samples was 3 percent. I have sampled approximately 1 m^3 volumes in 12 different snow layers using both 0.5 x $10^{-3}m^3$ and 2.3 x $10^{-3}m^3$ sample tubes. There was no difference between the results obtained with the different tubes, and the mean coefficient of variation was 10.8 percent. Leaf[1] found that, in volumes of 20 m^3, the coefficient of variation of water equivalent was 18 percent. Since the measurement of water equivalent includes both depth and density variations, we can conclude that the variability of snow density within a volume of tens of cubic meters is not much larger than the variability within a volume of 1 m^3.

Although the data are insufficient, it appears that samples taken from snowpits near avalanche starting zones will provide adequate measures of the densities of snow layers in the starting zones. It also appears that samples should be taken as widely spaced as possible within the pit to insure representative data.

Brittle Tensile Strength

There is an obvious relationship between the density of snow and its strength. Since the pores in snow cannot support any load, the entire load must be supported by the ice network. On a microscopic scale, tensile strength samples would range between zero, for air, and the maximum tensile strength of monocrystalline ice.

Unlike density, the tensile strength of a large volume of snow will not be the mean of a large number of random, microscopic subsamples. Problems arise in determining the distribution of stresses within a snow sample, but the major complication is that once part of the ice network fails, an increased load is thrown onto the remainder and the whole sample is very likely to fail. Thus, the strength of a large sample would not be the mean of the strengths distributed throughout the sample volume, but would be the minimum of the strengths distributed throughout the ice network. Put another way, we are of necessity sampling for an estimate of the minimum strength.

Suppose that the strength of a large volume ($\sim$1 m^3) of snow could be measured, then the volume broken up into smaller volumes ($\sim 10^{-3}m^3$) (without disturbing the distribution of strengths) and the strengths of the smaller volumes measured. The strength of the larger volume would not be the mean of the strengths of the smaller volumes, but would be the extreme low value found among them.

Cracks progagate through the entire slab thickness, which normally has a mean of about 1 m (Perla 1971). Stress gradients parallel to the slope are scaled to the slab thickness (Perla 1971, Smith 1972) so that a volume of about 1 m^3 seems to be the appropriate volume for strength considerations. Obviously, volumes of this size would be extremely difficult to test. We are then faced with the problem of determining the strengths of these large volumes of snow from smaller samples.

Fortunately, this problem is not unique to snow. A considerable amount of work has been done on strength problems of the type where there is a significant variation in the strengths distributed throughout a volume. The arguments given above are essentially those of Weibull (1939) who considered the general problem of the strength of nonuniform materials. Strength theories of this kind have the graphic name "weakest link" theories, apparently from the statement of Pierce (1926): "It is a truism, of which the mathematical implications are of no little interest, that the strength of a chain is that of its weakest link."

Weibull (1939) proposed the cumulative distribution function

$$F(\sigma) = 1 - e^{-V\left(\frac{\sigma-\sigma_u}{\sigma_o}\right)^m}, \quad \sigma \geq \sigma_u \qquad [1]$$

where σ is the applied stress, V the volume, and σ_u, σ_o, and m are material constants. This distribution is truncated in that the probability of failure at stresses below σ_u is zero.

[1]Personal communication with Charles F. Leaf, Rocky Mountain Forest and Range Experiment Station, Fort Collins.

Snow is seriously weakened by large voids within snow layers, which appear to be formed during snow deposition. I have observed voids of approximately $10^3 mm^3$. Some measure of the size and frequency of these larger voids can be gained from a comparison of centrifugal tensile tests performed using two different sample diameters. Keeler and Weeks (1967), Keeler (1969), and Martinelli (1971) performed a total of 592 tests using a sample 60 mm in diameter. They reported that about 10 percent of their samples showed zero strength. Some of the zero strengths may have been due to sample damage, but some undoubtedly resulted when a void cut entirely across the specimen. In contrast I have performed 338 tests using 120 mm samples without observing any zero strengths (Sommerfeld and Wolfe 1972). Thus, voids above 100 to 150 mm in diameter are very rare or nonexistent within snow layers, supporting the idea that the strength distribution is truncated.

Although the voids probably act as stress concentrators in their vicinity, the stress is supported by the surrounding material. When a sample tube cuts a void, part or all of the surrounding material is left behind and a spuriously low strength is measured. Thus, we have the problem that the most important values are seriously disturbed by the sampling technique. Furthermore, the number of very low strength elements in a large volume is so low that we have no assurance we have sampled the lowest strength in a given volume unless we sample the entire volume.

An alternative method of predicting the strength of a large volume of snow comes from Weibull's distribution (equation 1). If all but the few lowest sample values of snow strength (which may be erroneous as discussed above) in a limited density range are fitted to Weibull's distribution, the constants and particularly σ_u can be determined. At very large V the function $F(\sigma)$ (equation 1) jumps from zero at $\sigma = \sigma_u$ to almost 1 at stresses just above σ_u. Thus, σ_u should be the large-volume strength. Figure 1 shows the theoretical infinite volume curve in comparison with an experimental curve obtained with sample volumes of $2.3 \times 10^{-3} m^3$.[2] It appears that a volume of 1 m^3 would fall very close to the infinite volume curve.

[2]The reduced stress (σ/σ_m) used in this plot eliminates the effect of density differences among the samples (Sommerfeld 1971).

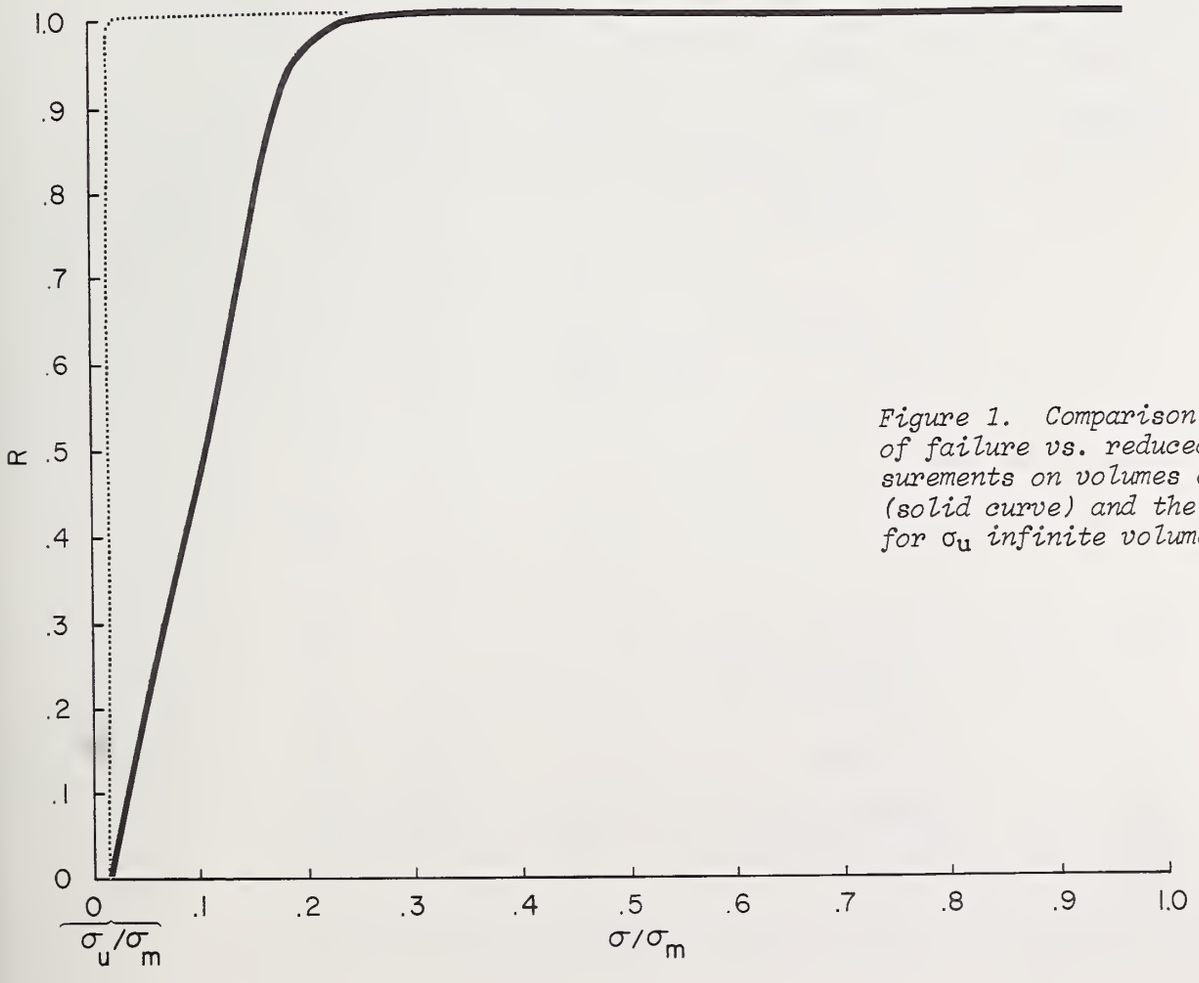

Figure 1. Comparison of the probability of failure vs. reduced stress for measurements on volumes of $2.3 \times 10^{-3} m^3$ *(solid curve) and the theoretical curve for* σ_u *infinite volume.*

To determine σ_u from centrifugal tensile tests, Weibull (1939) suggests the function

$$\ln \ln \frac{1}{1 - P} + \tfrac{1}{2} \ln \sigma = (m + \tfrac{1}{2}) \ln(\sigma - \sigma_u) + A(V) \qquad [2]$$

where P is the experimental probability of failure at stress σ and A(V) is a function of the sample volume. Equation 2 plots as a family of parallel curves, with different intercepts for different volumes. σ_u is determined as the unique value which gives the best fit to a straight line with $m + \frac{1}{2}$ as the slope.

Table I gives the calculated minimum strengths for various densities and types of snow. The snow was classified according to the scheme of Sommerfeld and LaChapelle (1970). Figure 2 shows σ_u plotted against mean density with the crystal type indicated at each point. In each case the lowest three strength values were discarded, since these values may be spuriously low, as previously discussed. In every case but the graupel (data group 11) the fit to the straight line was improved. In every case the fit to a straight line was very good, the lowest R^2 being 0.965 (fig. 3). A good fit to a straight line shows that the data fit the Weibull distribution very well. Of interest is the fact that the series which represents the normal course of equi-temperature metamorphism (1, 2, 4, 5, 6) falls on a very good straight line in figure 2. Because case 3 was somewhat windblown and 9 was heavily windblown, they might be expected to show higher strengths for their densities due to mechanical reworking. Cases 7 and 8 are dry, temperature-gradient (TG) snow and 10 is wet TG snow. Here we see that the strength of a TG layer can vary over a large range, which is supported by field observations. Graupel (11) gives a lower strength, which also agrees with the observations of Perla (1971).

TABLE I

DENSITIES AND CALCULATED MINIMUM STRENGTHS (σ_u) FOR VARIOUS TYPES OF SNOW

Case Number	Snow Type	Ave. ρ Kgm^{-3}	σ_u dynes cm^{-2}
1	IA (P1e, P1f)	112	5.38×10^3
2	IIB2	254	14.24×10^3
3	IB (I 3aN2A)→IA1	128	9.53×10^3
4	IIA 1 - 2	147	9.32×10^3
5	IIA 1 - 2	228	14.15×10^3
6	IA (P2s)	73	4.12×10^3
7	IIIB3	281	15.58×10^3
8	IIIB 2 - 3	242	4.04×10^3
9	IB (I1)→IIB2	289	36.81×10^3
10	IIIB3→IVA1	331	20.69×10^3
11	IA (IR3b, 4a, 4b)	249	5.60×10^3

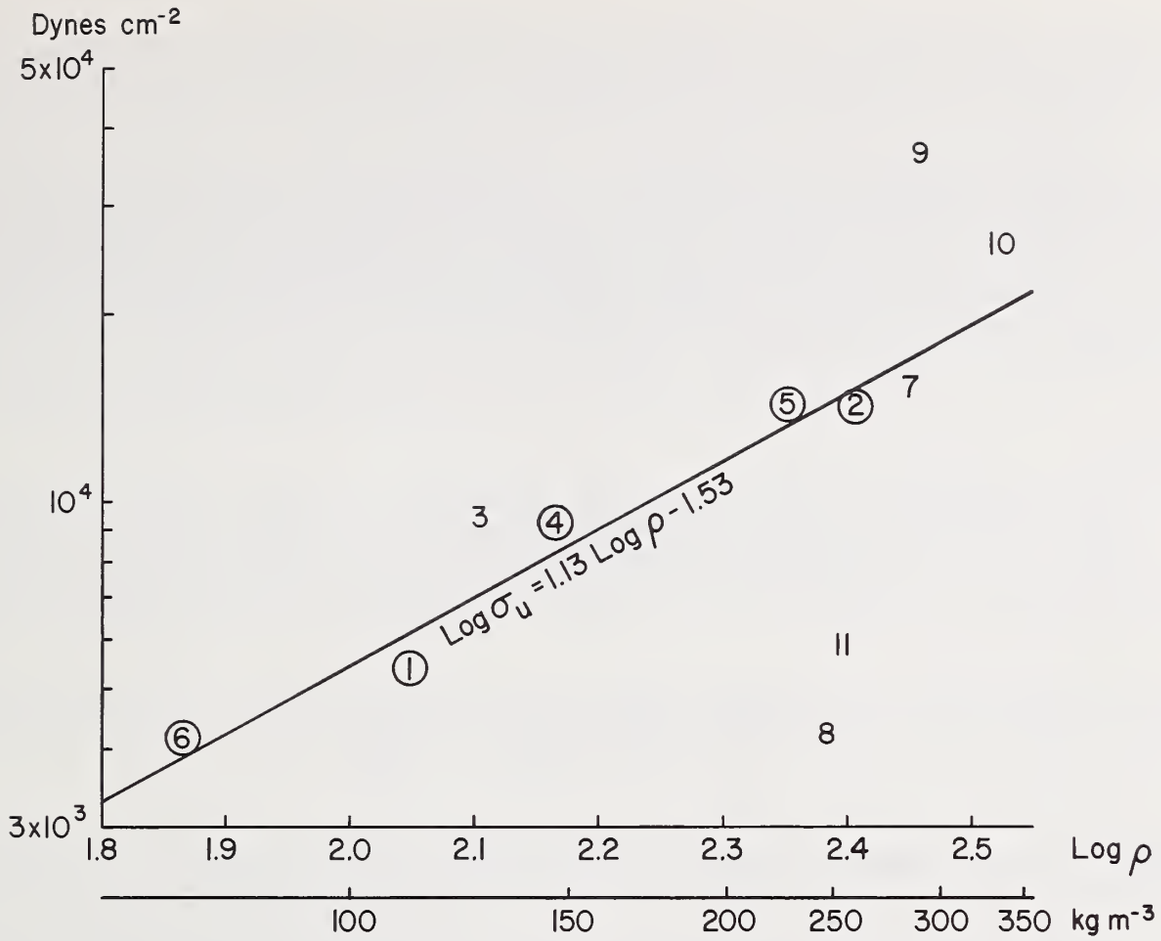

Figure 2. Calculated minimum strengths (σ_u) vs. density for various types of snow.

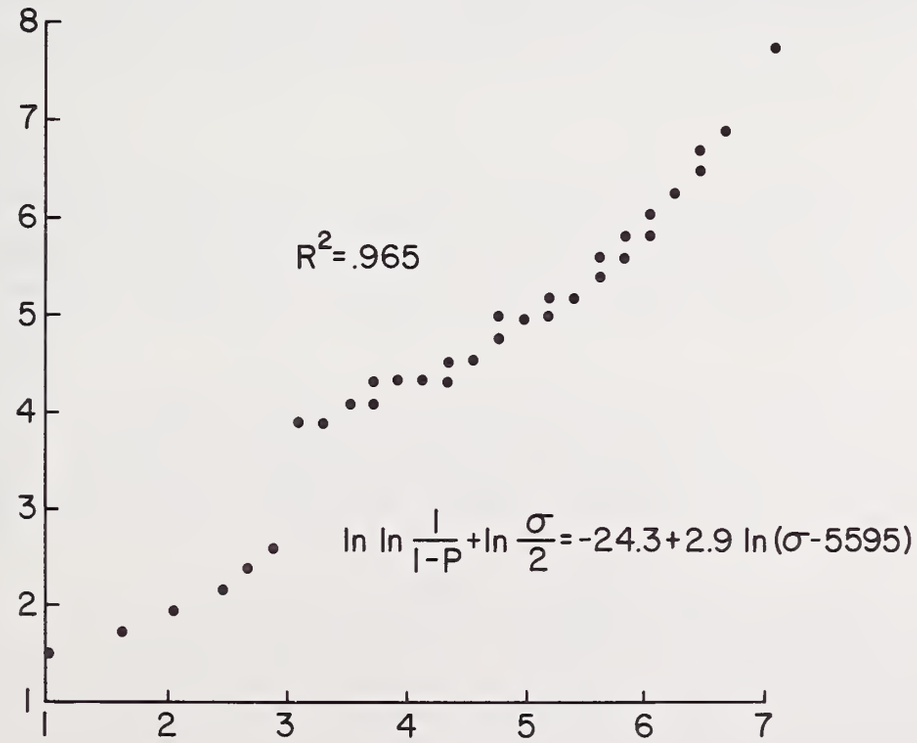

Figure 3. The worst fit of the data (case 11) to equation 2.

There are also similar but not so pronounced regularities exhibited by the other two constants. However, whatever meaning might be ascribed to such regularities is still a matter of conjecture.

Weibull's method as applied here boils down to assuming a distribution function (apparently chosen by Weibull for mathematical tractibility) that determines a set of constants from a set of data points, and uses the final function to extrapolate to an extreme limit. Undoubtedly such extrapolations are risky, but until data are available on the large-volume strengths of snow, this seems to be our only recourse. At least the Weibull analysis of the data leads to a fairly simple representation of the brittle tensile strength of snow, and that representation is consistent with other observations.

Shear Strength

Shear-strength measurements show characteristics similar to tensile-strength measurements (fig. 4). There is very large scatter in the data, but the measurements appear to fall between two extreme limits. Also, the larger the sample volume, the lower the mean of the measurements.[3] Here again the statistics of Weibull could be applied to determine σ_u for the shear strengths of various types of snow.

---

[3]Personal communication with Ronald I. Perla, Rocky Mountain Forest and Range Experiment Station, Fort Collins.

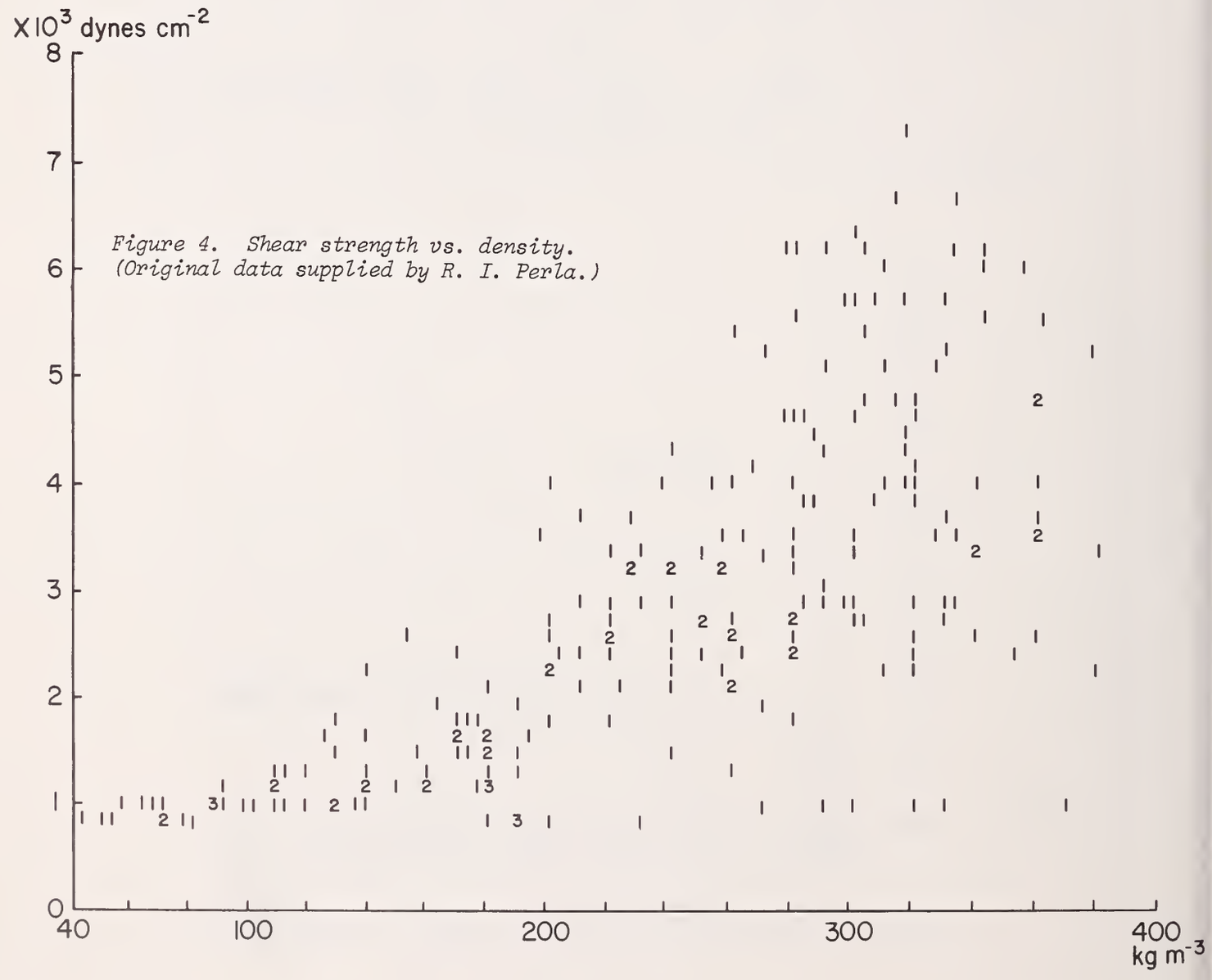

Figure 4. Shear strength vs. density. (Original data supplied by R. I. Perla.)

The assumption that avalanches are initiated by brittle shear crack propagation in the bed surface is open to question. During the formation of a tensile crack, the crack walls physically separate and the crack can become unstable and propagate in the manner of a Griffith (1921) failure. During shear failure, the failing parts are in contact, and friction and crack healing due to new bond formation impede crack growth. For these reasons a quasi-failure (Perla and LaChapelle 1970) is the likely initiating event. There is a strong possibility that a failure in a small part of the bed surface would not propagate elastically, and that the whole bed surface would not fail. Under such circumstances Weibull's statistics are not applicable, and the work of Daniels (1945), who considered the strengths of bundles of threads, appears to apply. Clearly the failure, at a particular stress, of one thread of a bundle may or may not lead to failure of the entire bundle depending on the strengths of the rest of the threads. Daniels showed that if $\theta(\sigma)$ is the probability density of the breaking stress (σ) of n elements, then a total load (S) is related to the load on each surviving thread (s) by

$$\frac{S}{n} = s \int_{s}^{\infty} \theta(\sigma) d\sigma \qquad [3]$$

and total failure occurs at the maximum

$$\frac{d\left[\frac{S}{n}\right]}{ds} = 0 = \frac{d}{ds} \left\{ s \int_{s}^{\infty} \theta(\sigma) d\sigma \right. \qquad [4]$$

s_T, the value of s at failure, can be found from the probability density function, and S_T/n, the stress at failure, can then be calculated.

The probability density function for snows of different densities can be derived from Perla's measurements.

The shear strengths measured by Perla for densities between 250 and 300 kg m^{-3} were found to fit the normal distribution with a mean of 30.0×10^3 dynes cm^{-2} and a standard deviation of 15.0×10^3 dynes cm^{-2}. Performing the calculations as in equations 3 and 4, we see that the failure stress for an entire layer within this density range, under our assumptions, is 15.8×10^3 dynes cm^{-2}, about 53 percent of the mean value.

Conclusions

The release of a slab avalanche is a complicated process. It appears that the initiation involves a volume of snow in the range 1 to 10 m^3. Field work indicates that it is necessary to interact with a volume of this size, with explosives, skiis, snowshoes, etc., to initiate an avalanche. Most slabs are about 1 m thick, and stress gradients parallel to the slope are scaled to the slab thickness, again indicating that a few cubic meters is the volume of interest for predicting slab failure.

Density is an important characteristic of snow slabs. The stresses within the slab are a direct result of the snow weight, and the mechanical properties of snow are related in basic ways to the snow density. Density is determined by the mean value of representative samples taken within a major layer. Available measurements are not conclusive, but do indicate that the density of 1 m^3 of snow in a major layer adequately represents the density of that layer.

The failure at the crown of a slab avalanche is undoubtedly brittle tensile fracture (Sommerfeld 1969), but the brittle tensile strength of snow cannot be understood in such simple terms as the density. The relationship of tensile strength to density is clarified by the application of "weakest link" strength theories. In particular, the statistics of Weibull (1939) give a consistent picture of the strength of a large volume of snow. It appears that the volume of interest in avalanche prediction (1 to 10 m^3) is large enough to be considered an infinite volume, and in that case the parameter σ_u in the Weibull distribution (equation 1) should be the snow strength. This strength has been shown to be a function of density for snows which have followed the normal course of equi-temperature metamorphism. Heavily windblown snow and temperature gradient snow need further study before their strength relationships become clear.

An important point which has been ignored in this study is the significance of the very large voids caused by rocks and vegetation which penetrate the slab. I know of no work on this subject, so at the moment nothing can be said concerning its importance.

The statistics of the shear strength of snow appear even more complicated. Since the failure of a part of the bed surface may or may not initiate the failure of the entire surface, the statistics developed for the evaluation of the strengths of thread bundles may be appropriate. In a limited test, measured shear strengths (in the density range 250 - 300 kg m^{-3}) were found to fit a normal distribution. Application of the statistics of Daniels (1945) for the large-volume case indicated that the bed surface should fail at about 53 percent of the mean shear strength of snow in that density range.

A complication which was ignored in the analysis is the time dependence of the shear strength of a snow layer. If a small part fails without initiating total failure, the snow in that part can rebond and the failure heal. This rate process might be included by making the shear strength distribution time dependent, but this has not been attempted.

Literature Cited

Daniels, H. E.
1945. The statistical theory of the strength of bundles of threads I. R. Soc. London Proc., Ser. A, 183:405.

Griffith, A. A.
1921. The phenomena of rupture and flow in solids. Philos. Trans. R. Soc. London, Ser. A221, p. 163-198.

Keeler, C. M.
1969. Some physical properties of alpine snow. U. S. Cold Reg. Res. Eng. Lab., Res. Rep. 271, 67 p. Hanover, N. H.

Keeler, C. M., and W. F. Weeks.
1967. Some mechanical properties of alpine snow, Montana 1964-66. U. S. Cold Reg. Res. Eng. Lab., Res. Rep. 227, 56 p. Hanover, N. H.

Martinelli, M., Jr.
1971. Physical properties of alpine snow as related to weather and avalanche conditions. USDA For. Serv. Res. Pap. RM-64, 35 p. Rocky Mt. For. and Range Exp. Stn., Fort Collins, Colo.

Perla, R. I.
1971. The slab avalanche. Ph.D. thesis, 101 p. Dep. Meteorol., Univ. of Utah, Salt Lake City, Utah.

Perla, R. I., and E. R. LaChapelle.
1970. A theory of snow slab failure. J. Geophys. Res. 75:619-627.

Pierce, F. T.
1926. Tensile tests for cotton yarns v. "The Weakest Link" - theorems on the strength of long and composite specimens. J. Text. Inst. 17:355.

Smith, F. W.
1972. Elastic stresses in layered snowpacks. J. Glaciol. 11:407-414.

Sommerfeld, R. A.
1969. The role of stress concentration in slab avalanche release. J. Glaciol. 8:451-462.

Sommerfeld, R. A.
1971. The relationship between density and tensile strength in snow. J. Glaciol. 10:357-362.

Sommerfeld, R. A., and E. R. LaChapelle.
1970. The classification of snow metamorphism. J. Glaciol. 9:3-17.

Sommerfeld, R. A., and F. Wolfe, Jr.
1972. A centrifugal tensile tester for snow. USDA For. Serv. Res. Note RM-227, 4 p. Rocky Mt. For. and Range Exp. Stn., Fort Collins, Colo.

Weibull, W.
1939. A statistical theory of the strength of materials. Ingeniorsvetenskapsakademiens, Handlingar 151-153, 45 p.

CONTROLLED RELEASE OF AVALANCHES BY EXPLOSIVES

Malcolm Mellor

ABSTRACT

The effects of explosives and blasting agents on snow are discussed from the viewpoint of rock-blasting technology. Air-blast, crater formation, and ground motion are considered, and the characteristics of various types of explosives are outlined. Recent developments in the commercial manufacture of liquid and slurried explosives and blasting agents are described, and the possibilities for application of these materials in avalanche control are explored.

Introduction

Explosives have long been used for deliberate controlled release of avalanches, using charge emplacement techniques that evolved to suit prevailing conditions. The principal methods of charge emplacement have been: i) hand delivery, in which solid charges are laid on the snow surface or thrust into the snowpack for immediate firing, and ii) projectile delivery, in which fuzed charges are fired into the target zone by guns. Consideration has been given to emplacement of explosive charges prior to winter for firing on demand, but this technique is probably unacceptable in areas where there is unrestricted public access.

Established methods appear to be reasonably effective, although from a technical standpoint there are some questionable aspects and quantitative information is very limited. From a safety standpoint, the record for avalanche blasting is very good, but safe application of traditional methods seems to depend heavily on the skill and integrity of control personnel; by contrast, industrial applications of explosives demand inherently safe procedures.

The following notes are intended to review the behavior of explosives and blasting agents, the response of snow to explosives, and recent developments that might be applicable to avalanche blasting. One objective of this review is to bring out the great difference in response characteristics between snow and the materials for which typical blasting technology has been developed.

Action of Explosives

An explosion involves very rapid generation of energy in limited space, with sudden development of great pressure, usually accompanied by violent gas expansion. It is commonly created by direct chemical reaction, but other thermal, mechanical, electrical, or nuclear processes can give rise to explosions when energy is released at rates greatly exceeding the local dissipation rate. In a chemical explosive a great amount of energy – approximately 1 kcal/g – is released in a very short time (microsecond reaction time), so that the power level is enormous (about 50 billion kilowatts per square meter at the detonation front).

Chemical explosives undergo exothermic reaction, propagating a reaction wave from the point of initiation. If the velocity of this wave is higher than the acoustic velocity of the unreacted material, as in "high" explosives, the process is called *detonation*; if it is lower than the acoustic velocity of the unreacted material, as in "low" explosives or propellants, it is called *deflagration*. Ideal detonation velocities of some explosives exceed 8000 m/sec. Detonation pressure (which can exceed 300,000 atmospheres in some explosives) is approximately proportional to the square of

detonation velocity, and therefore explosives with high detonation velocity can be expected to produce intense shock waves and to have great shattering power, or brisance. By contrast, deflagrating explosives such as black powder are unlikely to transmit a true shock wave to surrounding material, and they depend almost entirely on gas expansion for their blasting effectiveness.

Gas blasting can also be accomplished with devices other than conventional chemical explosives. Air-blasting systems release high pressure air (typically around 12,000 lbf/in.^{2}) from containers charged by multi-stage compressors. Carbon dioxide systems vaporize liquid CO_2 by a heater element and discharge it from a shell at high pressure. Fuel/oxidant devices explode gas or vapor mixtures (e.g. propane and compressed air) in a combustion chamber and discharge through a venting port.

When fired inside a solid or fluid medium, a high explosive creates a severe stress wave, or shock wave, which initially propagates radially outward from the charge at a speed higher than the acoustic velocity of the medium. Geometrical spreading and losses in the medium cause the wave to attenuate rapidly, reducing both amplitude and velocity until it eventually becomes an elastic wave traveling at the sonic velocity of the medium. The initial amplitude of the shock wave from a typical high explosive far exceeds the yield strength of any solid material, and material in the immediate vicinity of the charge undergoes intense compression that is essentially hydrodynamic and adiabatic; brittle material such as rock is completely pulverized in this zone. As distance from the charge increases, plastic or inelastic compression becomes progressively less severe, and shear resistance of the confining material becomes increasingly important. At greater ranges, where wave amplitude drops below the elastic limit of the medium, tensile hoop stresses (tangential stresses) associated with the radial pressure pulse cause radial cracking. When the radial stress wave meets free boundaries (rock/air interfaces) at normal incidence it reflects as a tensile wave, and surface spalling will occur if the amplitude is great enough.

In many materials only a minor proportion of the total explosive energy is transmitted in the shock wave – typically less than 20% in common rocks, and sometimes only a few percent. For a given type of explosive, the initial shock intensity in a solid medium is governed largely by the efficiency of coupling between the explosive and the medium. Good coupling calls for intimate contact between the charge and the medium (as with a liquid or slurry explosive), and for "impedance matching," i.e. for the product of detonation velocity and density for the explosive to be approximately equal to the product of acoustic velocity and density for the medium. Once the shock has been transmitted to the medium, a great deal of its energy is absorbed immediately in the hydrodynamic compression zone. The effectiveness of a given material in transmitting or absorbing shock energy in the hydrodynamic zone is characterized largely by the Rankine-Hugoniot equation of state, or by a graphical "Hugoniot" characteristic giving the pressure/volume relationship for very rapid loading and unloading. In broad terms, a material that is highly compressible over the applicable pressure range can be expected to be effective in attenuating shock pressure.

The spherical wave propagating from a point charge in an isotropic infinite medium attenuates geometrically, with wave amplitude inversely proportional to radius and wave energy inversely proportional to radius squared. The wave also attenuates because of internal energy dissipation in the medium, with amplitude decreasing exponentially with distance traveled. The combined attenuation is best described by a function with an inverse proportionality factor and an exponential decay factor, but in practice it is usual to plot shock pressure against scaled radius on logarithmic scales and express the result approximately as a simple power relation, with amplitude inversely proportional to radius raised to a power of roughly 2 to 3, depending on the material type and the radius (the power decreases with increasing scaled radius).

So far the discussion has been confined to the stress wave, which actually accounts for only a minor portion of the explosive energy. It is next necessary to consider the expanding gases which follow the stress wave and contain most of the available energy.

All chemical explosives produce large volumes of high pressure gas, and in typical blasting situations most of the explosive energy is utilized in expanding this gas. In an underwater explosion the expanding gas produces a bubble which displaces water radially outward, continuing to grow until its internal pressure drops below the ambient hydrostatic pressure and flow reverses. (In deep water, the bubble pulsates in size, and it rises and deforms by buoyancy effects.) When an explosion occurs deep inside a solid medium, the gas can only expand into the cavity formed by shock wave crushing, into cracks formed by the shock wave, into pre-existing cracks or pores, or into cracks that are formed by the gas pressure itself. The usual objective in blasting practice is to create a situation where the expanding gas can form and exploit cracks so as to displace material to a free boundary.

Low explosives and gas blasting devices set deep into strong impermeable material are often incapable of initiating cracks; they have to rely on existing flaws such as cracks, pores, planes of weakness, etc. However, they are particularly effective in situations where shock damage is either unnecessary or detrimental. For example, in blasting hard coal there is no necessity for stress wave shattering, and in "heaving" surface slabs, such as concrete pavements or floating ice, shock damage can produce premature venting of the gas, with consequent reduction of flexural breakage. For blasting strong uncracked rock in large masses it is usually more economical to use a high explosive, using the shock wave to initiate cracks that can be exploited and extended by the gases. For any type of explosive an air space between the charge and the solid medium can greatly reduce the initial gas pressure as well as shock wave amplitude, and an unstemmed shothole can similarly reduce the gas pressure that is applied to the blasted material.

In order to characterize the properties of explosives and the blast response of materials, it is convenient to scale shock and blast effects to remove the effect of charge size. In ordinary blasting practice, where body forces in the blasted medium are negligible, dynamic and geometric similitude permits linear dimensions such as charge depth, burden, hole spacing, crater radius, etc. to be normalized with respect to charge radius for a given type of explosive. For a given charge density the charge volume is proportional to charge weight, and thus it has become usual to scale linear dimensions with respect to the cube root of charge weight, i.e. a length measured in feet is divided by the cube root of charge weight measured in pounds to give a scaled length expressed in units of $ft/lb^{1/3}$.

Response of Snow to Explosives

Snow is very different from materials that are usually blasted by explosives; it is very weak, and can be excavated and handled with ease. However, the low strength and low density of snow do not lead to any great increase in blasting effectiveness, since snow is an energy-absorbing medium.

The coupling between a high explosive charge and snow is generally poor, and theoretically the impedance matching is far from ideal. The snow lying in avalanche starting zones is not likely to have acoustic velocities much above 1000 m/sec, and low density snow may have acoustic velocities of only a few hundred meters per second. Thus the product of acoustic velocity and snow density is likely to be an order of magnitude lower than the product of detonation velocity and density for explosives and blasting agents. By contrast, the impedance matching ratio for frozen soil is close to unity for typical explosives. In snow the hydrodynamic zone, in which energy is absorbed by inelastic compression of the material, is relatively large, as snow is readily compressible and a significant amount of compression is irreversible. Adiabatic compressibility curves (Hugoniot curves) show that snow of about 0.4 g/cm^3 density can be compressed to about 50% of its unstrained volume by pressures of only 20 bars or so.

Direct experimental evidence shows that dense snow, of the type found in the surface layers of the Greenland Ice Sheet, is tremendously effective in attenuating stress waves (Fig. 1). At close range, such as 1 ft from a 1-lb charge, the peak pressure in snow is much smaller than the

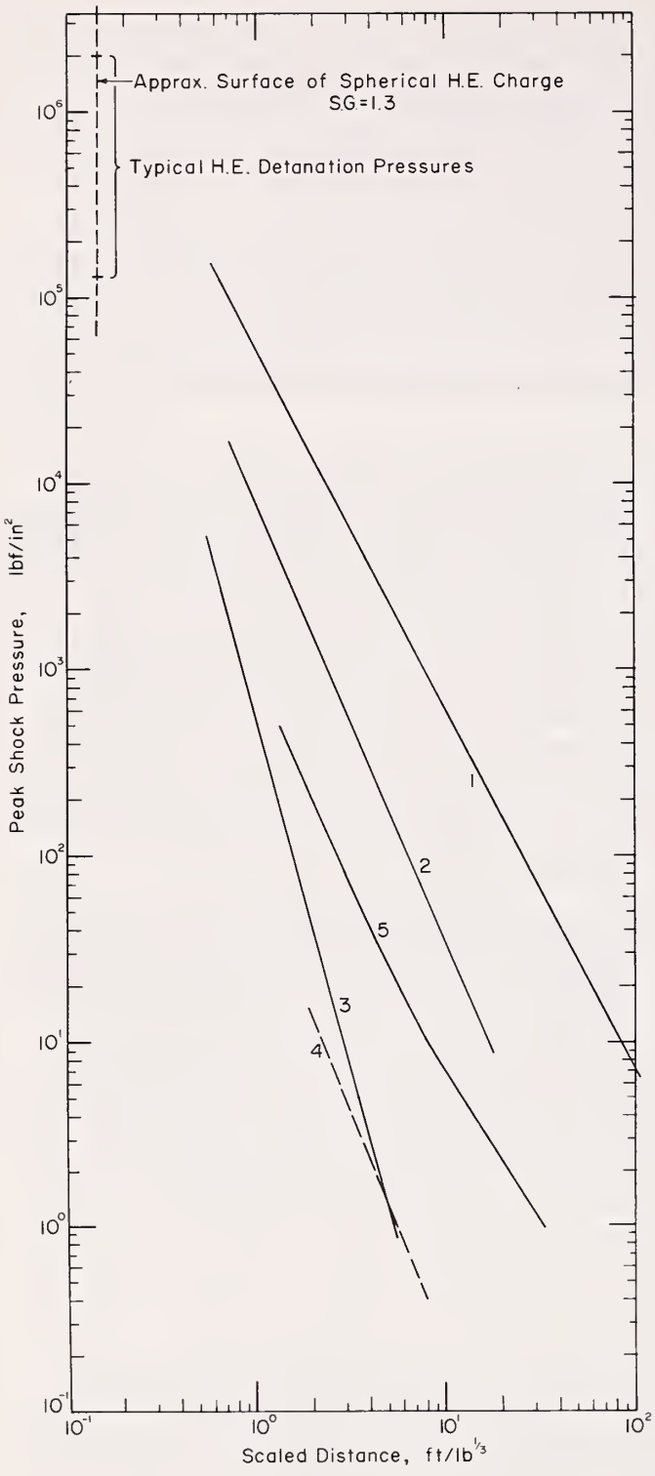

Figure 1. Stress wave attenuation in various materials. 1) Granite, 2) glacier ice, 3) ice cap snow, 4) seasonal snow, 5) air. (See Mellor 1968 and 1972 for details of data sources.)

corresponding pressure in granite – about 100 times smaller. Looking at the attenuation in relative terms, the scaled distance from the charge at which shock pressure drops below the uniaxial compressive strength of the material is shorter for snow than for granite.

The strong attenuating properties of snow become evident when explosive cratering capabilities are considered. In Figure 2 the dimensions of craters in dense snow are plotted against charge depth, all linear dimensions being scaled with respect to the cube root of charge weight. Comparative data for solid ice and frozen ground are given in Appendix A. In spite of the low density and low strength of snow, crater dimensions are very similar to corresponding dimensions for solid ice, and crater radius in snow is about the same as crater radius in frozen soils.

When a concentrated explosive charge is detonated in air above a snow surface a pressure wave propagates spherically, eventually making contact with the surface and reflecting from the surface. Reflection reinforces the pressure wave, but a snow surface is less effective than a rigid surface in producing this reinforcement. Figure 3 gives relationships between incident pressure and reflected pressure at normal incidence for a snow surface and a rigid surface. The reflected wave travels through air that has been compressed adiabatically by the incident wave, and since this allows it to travel faster than the incident wave it can overtake and fuse with the incident wave for a certain range of incidence angles, as illustrated in Figure 4. This effect causes the airblast pressure at the snow surface to vary with distance and with height of burst as shown in Figure 5.

Release of Avalanches by Explosives

The exact mechanism by which explosions release avalanches is not known, but some relevant factors can be identified.

First of all, an explosion propagates a stress wave that can travel through the air above the snow, through the snow itself, or through the ground beneath the snow. The stress wave abruptly displaces particles in the material it traverses, producing strains and accelerations. Secondly, the explosion generates a bubble of rapidly expanding gas that can thrust against confining material and can pressurize cracks and pores.

The general aim is to destroy the stability of an inclined layer of snow by increasing stress, by decreasing strength, or by a combination of the two.

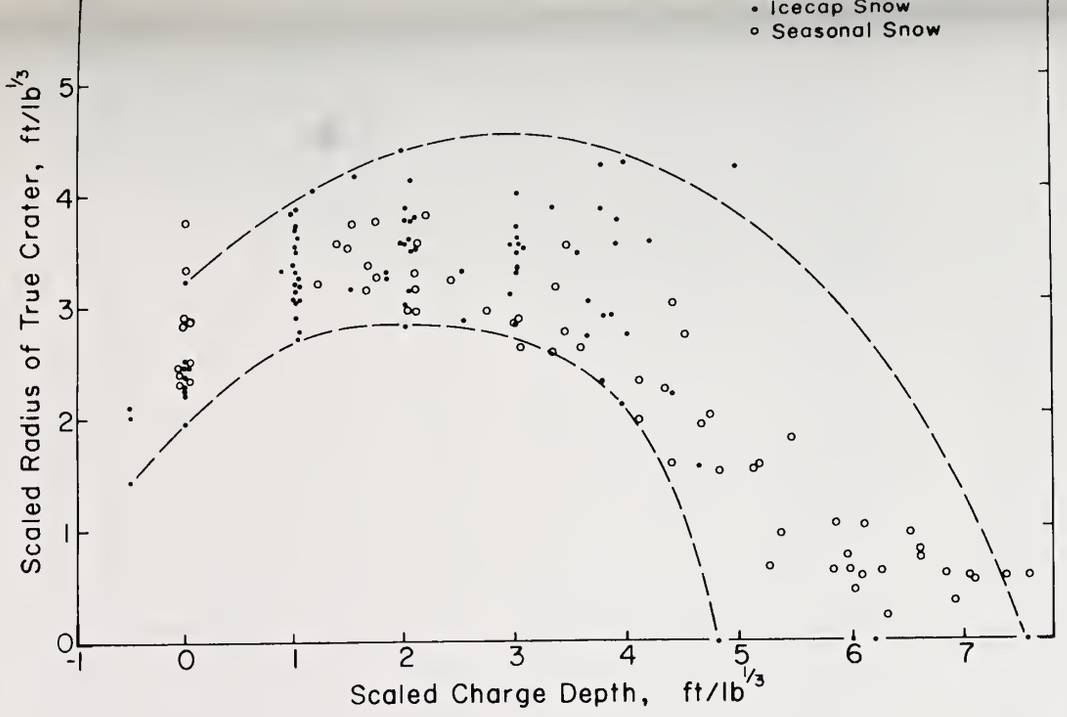

Figure 2. Scaled crater data for snow. (Basic data from Livingston 1968 and Fuchs 1957.)

b.

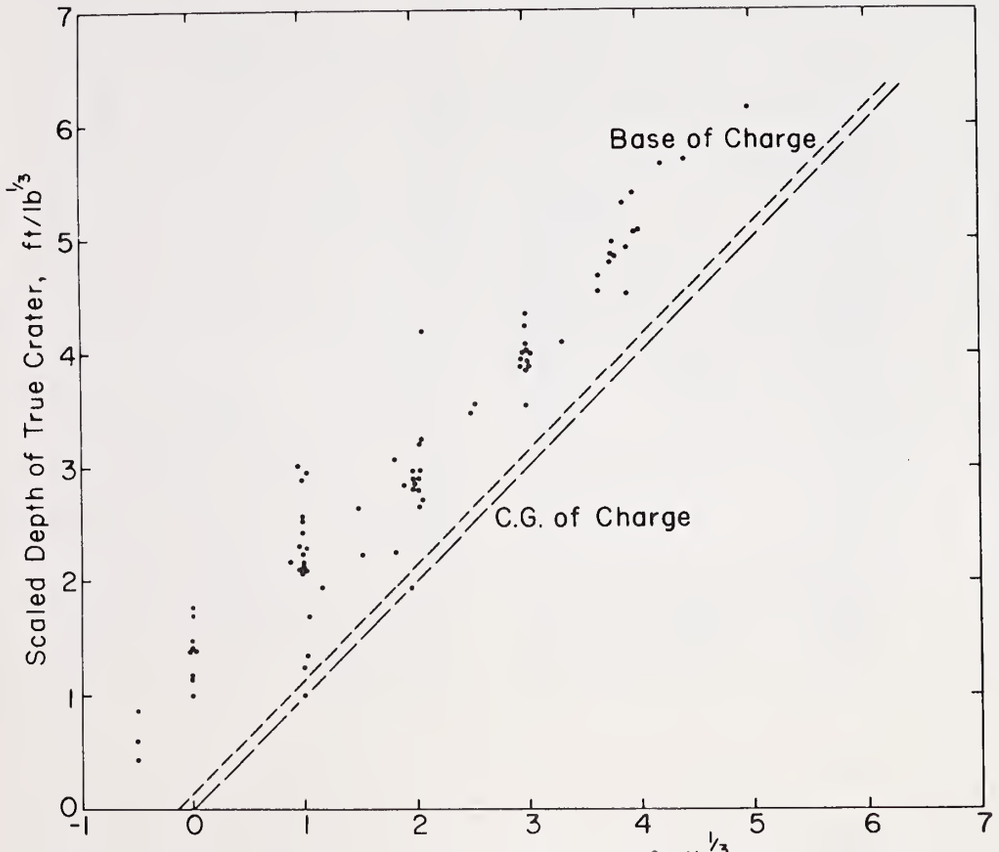

c.

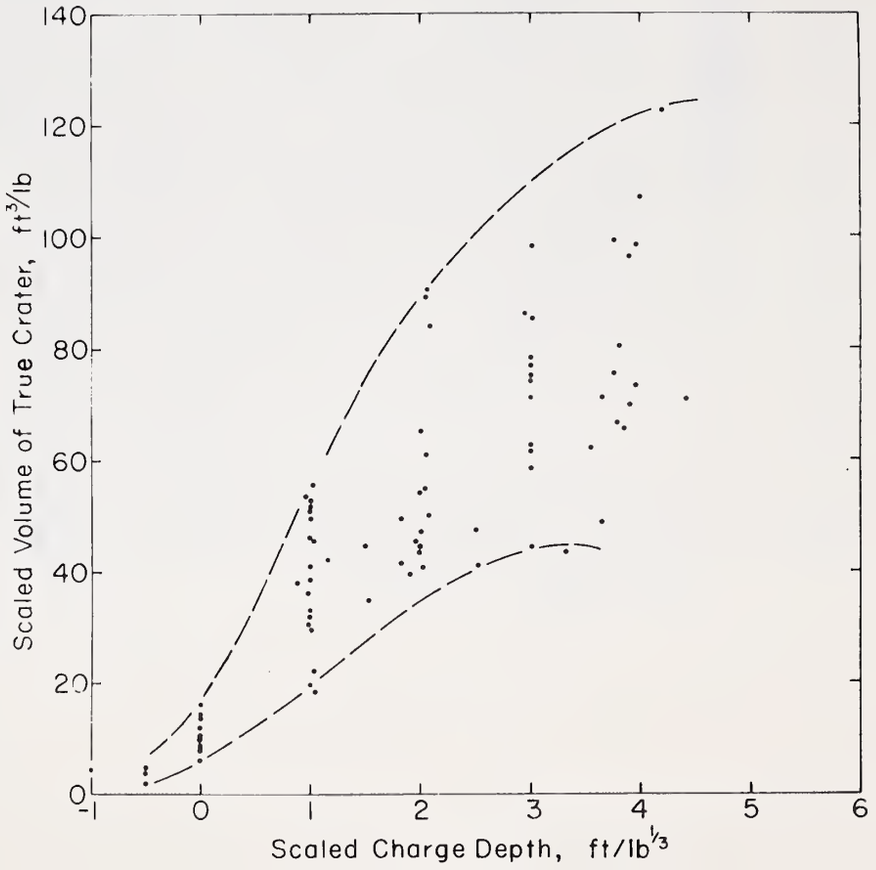

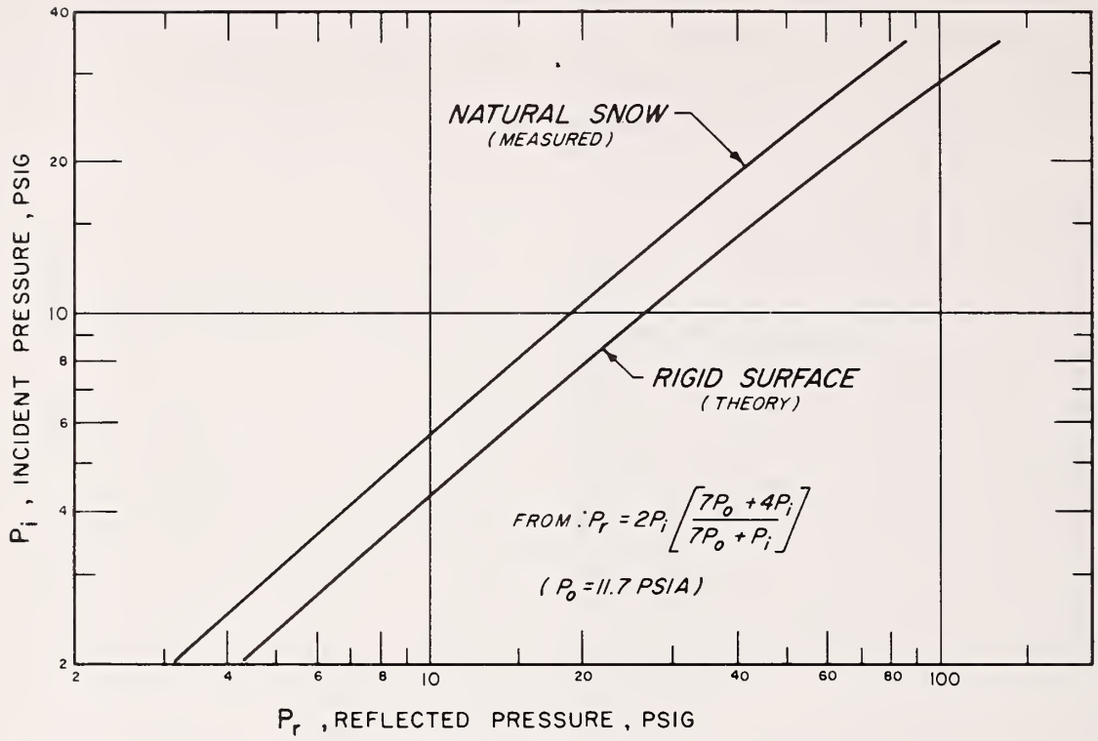

Figure 3. Relations between incident pressure and reflected pressure for normal reflection of airblast from a rigid surface and a snow surface. (From Ingram 1962.)

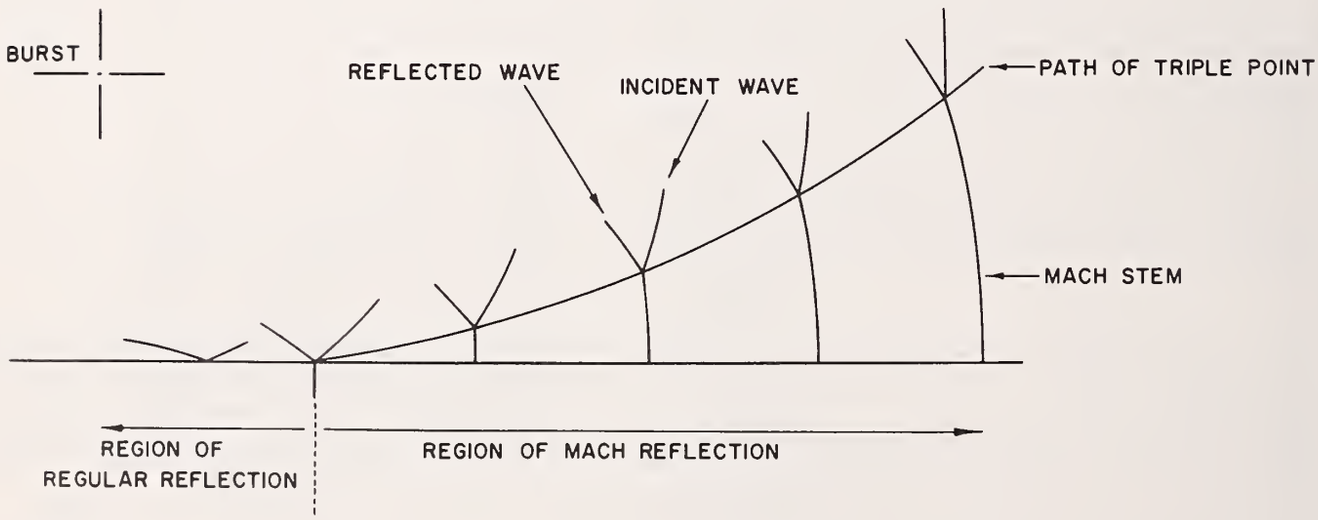

Figure 4. Wave fusion and mach front progression for airblast over a reflecting surface.

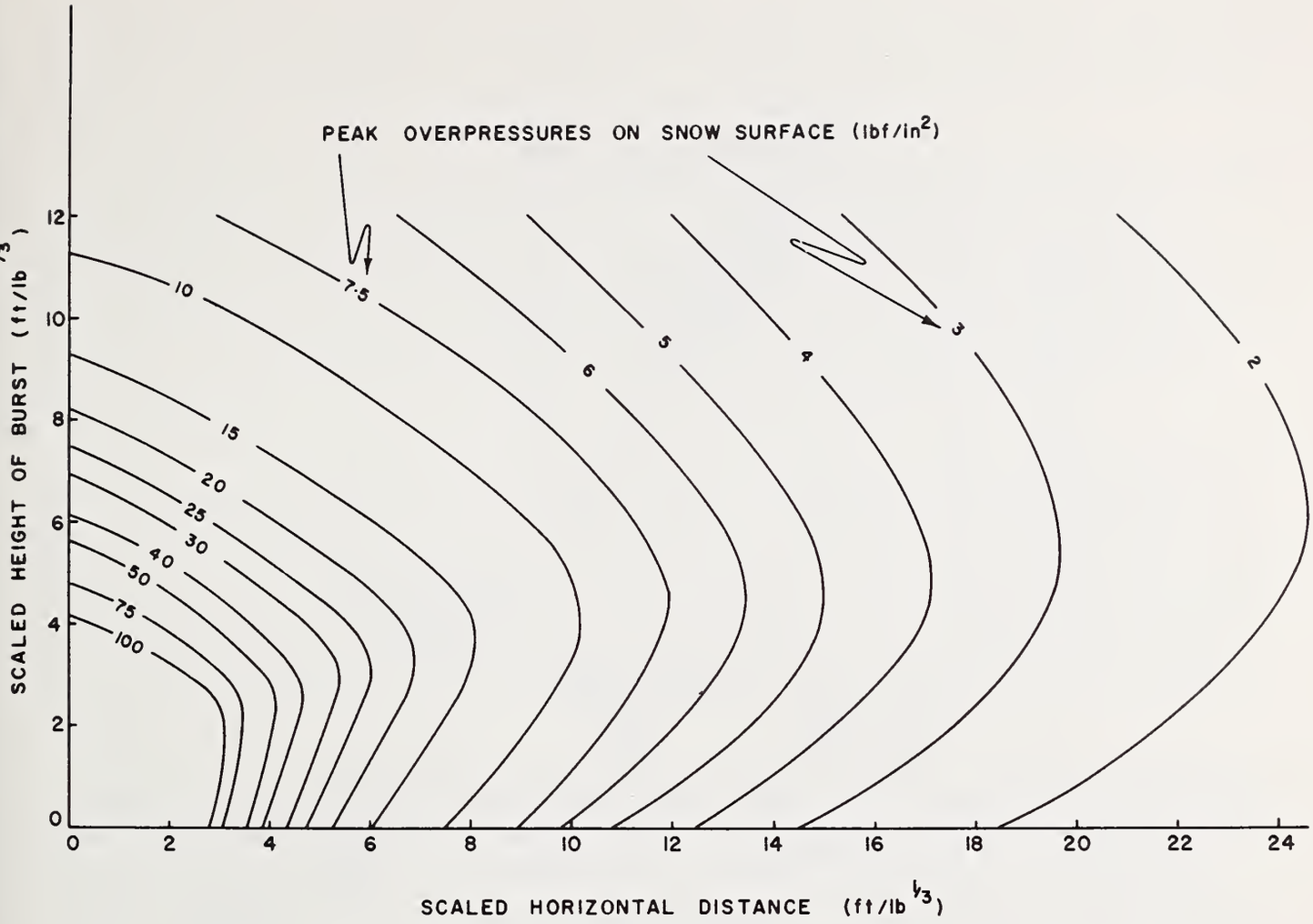

Figure 5. Peak overpressures related to height of burst and distance from ground zero for airblast over snow. (After Ingram 1962.)

One very positive method of attacking the snow slope, especially when it consists of a coherent slab, is to cut a swath in a direction normal to the fall line, thereby interrupting the continuity and at the same time applying downslope thrust, airblast, ground shock, and ejecta impact. This approach calls for either a line of point charges or a continuous linear charge, and there is no doubt that the charges should be set at optimum depth, which for practical purposes can be taken conservatively as 3 ft/lb$^{1/3}$ (striking a balance between maxima for crater radius and crater volume and allowing for variation of snow type). In practice, charges would probably be set within about 1 ft of the base of the snowpack, and optimum charge weight W_{opt} (lb) would be calculated for the actual overburden depth H (ft) using the relationship $W_{opt} = (H/3)^3$. A simple rule for estimating spacing of point charges would be to take spacing equal to twice the charge depth. This method is positive, but it is not economical and in many cases would amount to overkill.

A very different method is to apply airblast to the snow surface, thereby creating a brief (~ 10 msec) increase of normal stress and downslope shear stress. With this method much of the explosive energy is dissipated in air, but the loading is relatively widespread. A quantitative approach to airblast loading is difficult, since the release mechanism is not fully understood and the required overpressure varies considerably with the type of snow and its inherent stability. A simple way of looking at the problem is to consider the airblast as a transient normal pressure which at distant range translates to an increase of downslope shear stress and an increase of intergranular friction, the latter effect being partly offset by pressure rise in the pores of the snow (pressure rise in the pores lags and attenuates with increasing distance from the surface). Some indication of a lower limit of useful airblast overpressure is provided by sonic booms from aircraft, which sometimes release unstable snow with widespread overpressures of approximately 2 lbf/ft^2 (1.4×10^{-2} lbf/in.^{2}).

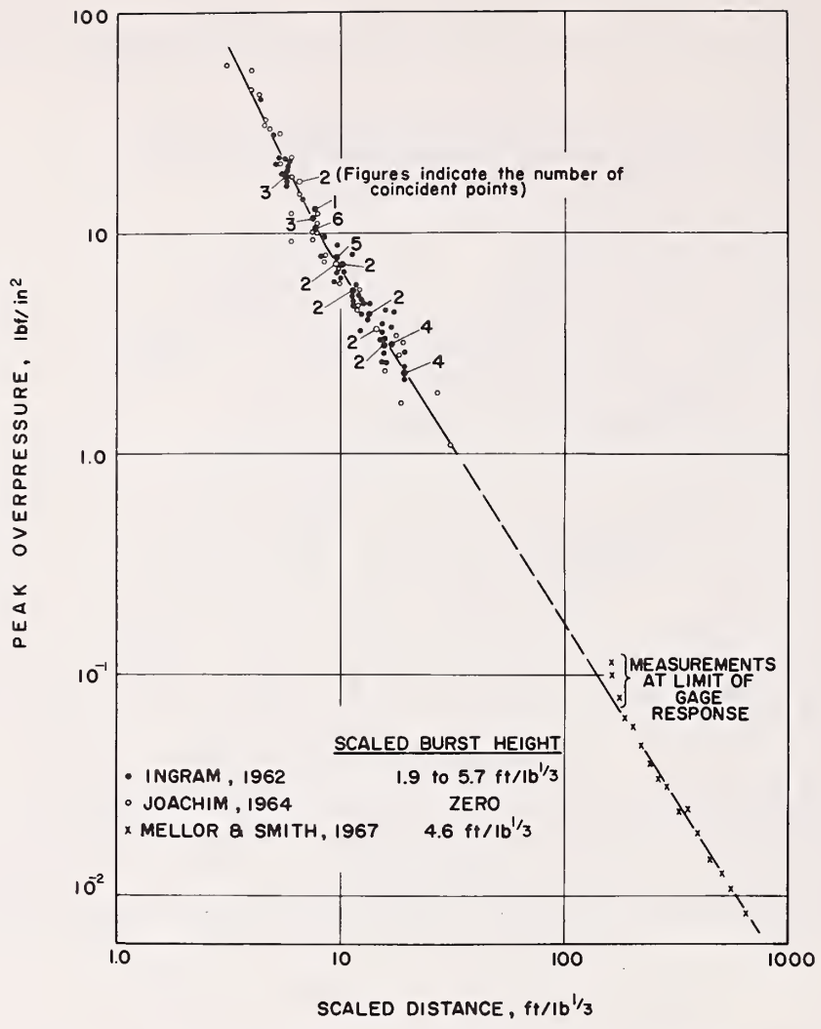

Figure 6. Airblast overpressure above a level snow surface (all data adjusted to 6000 ft altitude).

This pressure level is equivalent to rapid addition and removal of 4 to 5 in. of low density (0.1 g/cm^3) snow at typical release zone slope angles. For more positive results from airblast it might be better to plan on covering the target zone with at least 0.5 lbf/in.^{2}, which is rather higher than the nominal ground pressure of a man on skis. With a burst height of about 5 ft/lb$^{1/3}$, pressures exceeding 0.5 lbf/in.^{2} would spread to a radius of almost 50 ft/lb$^{1/3}$ (Fig. 6), i.e. a 1-lb charge fired about 5 ft above the snow surface would cover a target zone 100 ft in diameter, or an 8-lb charge fired at a height of about 10 ft would cover a 200-ft-diameter zone. With a charge fired at the snow surface, the coverage radius might be about 25% lower than the values given, but the charge will also form an appreciable crater (Fig. 2).

A third possibility is to fire charges at the base of the snowpack, using the underlying ground to spread the shock and limiting charge size so as to suppress venting and thereby utilize gas expansion within the snow cover. One potential advantage of this technique is that shock attenuation in rock is much less than in snow or air (Fig. 1), so that ground disturbance ought to be significant over a relatively wide area. The other feature is that gas expansion can be used to exploit planes of weakness and to pressurize the pores of the snow, the aim being to "heave" the snowpack and to lower the shear strength by increasing pore pressure. With this method, charges would be laid in contact with the ground and charge size would be scaled to give critical weight W_{crit} (lb) for the prevailing overburden H (ft) using the relationship $W_{crit} = (H/7)^3$.

Possibilities for Technical Developments

There are a number of possibilities for innovation in avalanche blasting, but it would be desirable to first make a systematic study of the relative effectiveness of airblast, hydrodynamic

disruption, undersnow shock, undersnow gas expansion, and ground shock. Without such information, it is difficult to assess various types of explosives and blasting devices, or to select optimum methods of charge emplacement or projectile fuzing. However, it may be worth mentioning some techniques that do not seem to have been tested for avalanche blasting.

Over the past decade there have been considerable developments in the production and use of explosives and blasting agents based on ammonium nitrate, particularly in slurry form, and there has been renewed interest in liquid explosives, especially those based on nitroparaffins and hydrazines. Some of these materials are blasting agents that contain no high explosive ingredients and are not cap-sensitive, while other materials consist of two separate non-explosive components that are blended into an explosive immediately before use. These characteristics permit the materials to be transported, handled and stored under more relaxed regulations than those that cover Class A explosives.

The availability of cheap and safe fluid explosives opens up some prospects for novel applications and emplacement techniques in avalanche work. For example, plastic pipes could be laid from a safe and sheltered standpoint to an avalance release zone before the first snowfall, and fluid explosive could be loaded hydraulically as required during the winter, using gravity flow or pumping. The blasting cap for each pipeline could be either pre-placed or in the charge chamber introduced with the hydraulic load. The charge chamber could be designed to give a concentrated charge, a linear charge, or a dispersed charge, and it could be set either at ground level or at the top of a post rising above snow level.

At places where frequent repetitive avalanche blasting is required in a limited area, such as at a mine site in the mountains, a permanent installation of compressed air blasting equipment might have operational and economic advantages. With this type of system reusable airblasting shells would be set at ground level in avalanche release zones, with high pressure lines running to a centrally located multi-stage compressor. The shells would fire automatically by remote control when a pre-set pressure level (around 12,000 lbf/in.^{2}) was imposed by the compressor. The blasting elements installed on the snow slopes would be completely inert until activated by the controller. Initial cost of such a system would be relatively high, but operating costs would be low.

The technical effectiveness of gas blasting could be tested easily and cheaply by using carbon dioxide shells, which themselves could be used as a substitute for explosives in a pre-placement system. These shells contain liquid carbon dioxide, which is vaporized and discharged when an electrically actuated heater element is fired.

There are possibilities for development of a cheaper system of repetitive blasting using direct combustion of gaseous fuel/oxidant mixtures such as propane and ordinary compressed air. A system of this type would probably have a combustion chamber permanently installed at the blasting site, with rechargeable storage tanks for fuel and oxidant nearby. The chamber would be charged for each firing by remotely operated valves, and would be fired electrically with a "spark plug."

Permanent installations for avalanche blasting can probably not be justified in most areas under present conditions, but it seems quite likely that increasing recreational and industrial activity in the mountains could change the situation in the future. Pushbutton systems would be less entertaining than hand-charging or artillery fire, but they might be safer and more positive.

References

Anderson, G.D. (1968) The equation of state of ice and composite frozen soil material. U.S. Army Cold Regions Research and Engineering Laboratory (USA CRREL) Research Report 257.

Fan, S.S.T. and Y-C. Yen (1968) Nonsteady one dimensional compressible fluid flow through anisotropic porous media. USA CRREL Research Report 256.

Fuchs, A. (1957) Effects of explosives on snow. U.S. Army Snow, Ice and Permafrost Research Establishment (USA SIPRE) Special Report 23.

Ingram, L.F. (1962) Air blast in an arctic environment. U.S. Army Waterways Experiment Station, Technical Report 2-597.

Ingram, L.F. and S.H. Halper (1960) Measurement of explosion-induced shock waves in ice and snow, Greenland, 1957 and 1958. U.S. Army Waterways Experiment Station, Miscellaneous Paper 2-399.

Ingram, L.F. and J.N. Strange (1958) Blast-pressure measurements in snow. U.S. Army Waterways Experiment Station, Miscellaneous Paper 2-274.

Joachim, C.E. (1967) Shock transmission through ice and snow. U.S. Army Waterways Experiment Station, Technical Report 1-794.

Livingston, C.W. (1960) Explosions in ice. USA SIPRE Technical Report 75.

Livingston, C.W. (1968) Explosions in snow. USA CRREL Technical Report 86.

Mellor, M. (1965) Explosions and snow. USA CRREL Cold Regions Science and Engineering Monograph III-A3a.

Mellor, M. (1968) Avalanches. USA CRREL Cold Regions Science and Engineering Monograph III-A3.

Mellor, M. (1972) Use of liquid explosives for excavation of frozen ground. Symposium on Military Applications of Commercial Explosives, Defence Research Establishment, Valcartier, Quebec.

Mellor, M. and N. Smith (1967) Airblast attenuation at low overpressures. USA CRREL Technical Note (unpublished).

Napadensky, H. (1964) Dynamic response of snow to high rates of loading. USA CRREL Research Report 110.

Smith, N. (1962) Air pressures and shock wave velocities from high explosive surface contact explosions over arctic snow surface. USA CRREL Technical Note (unpublished).

Smith, J.L. (1969) Shock tube experiments on snow. USA CRREL Technical Report 218.

Yen, Y-C. and S.S.T. Fan (1966) Pressure wave propagation in snow with nonuniform permeability. USA CRREL Research Report 210.

Appendix A. Crater Data for Ice and Frozen Ground

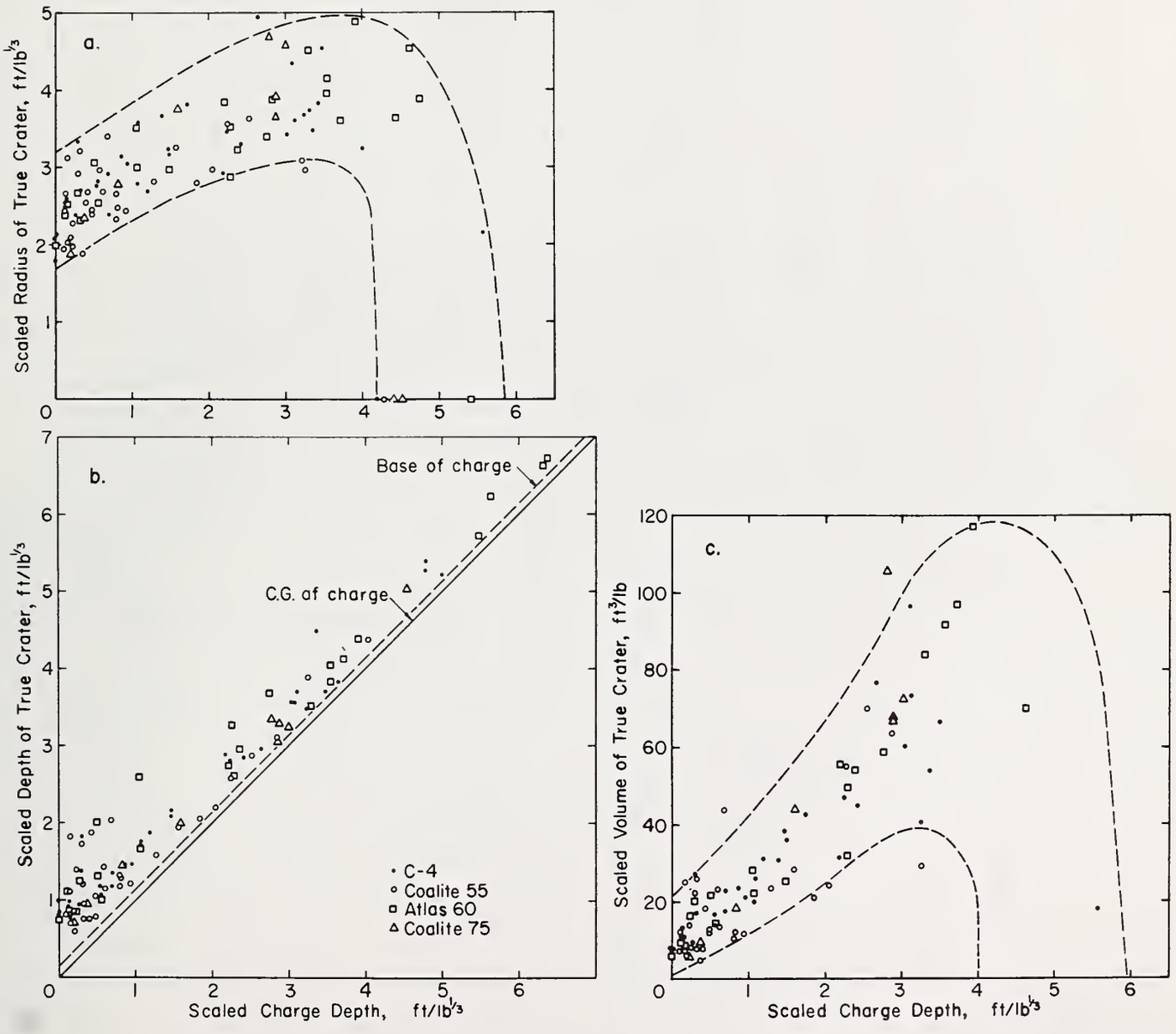

Figure A1. Scaled data for cratering blasts in massive glacier ice. (Scaled from test results by Livingston 1960.)

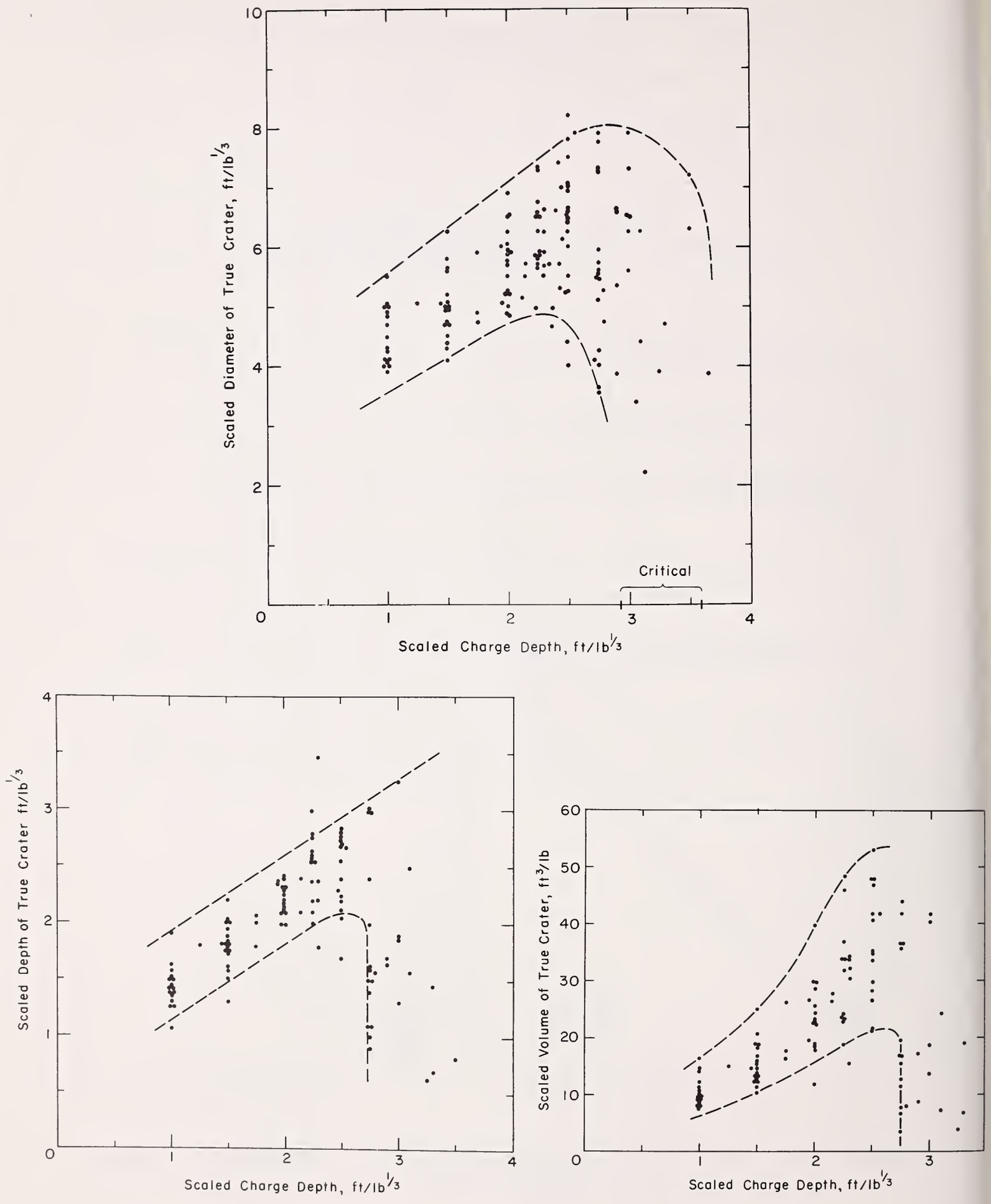

Figure A2. Scaled crater data for frozen silt. (Basic data from McCoy 1965, Mellor and Sellmann 1970, Mellor 1971.)

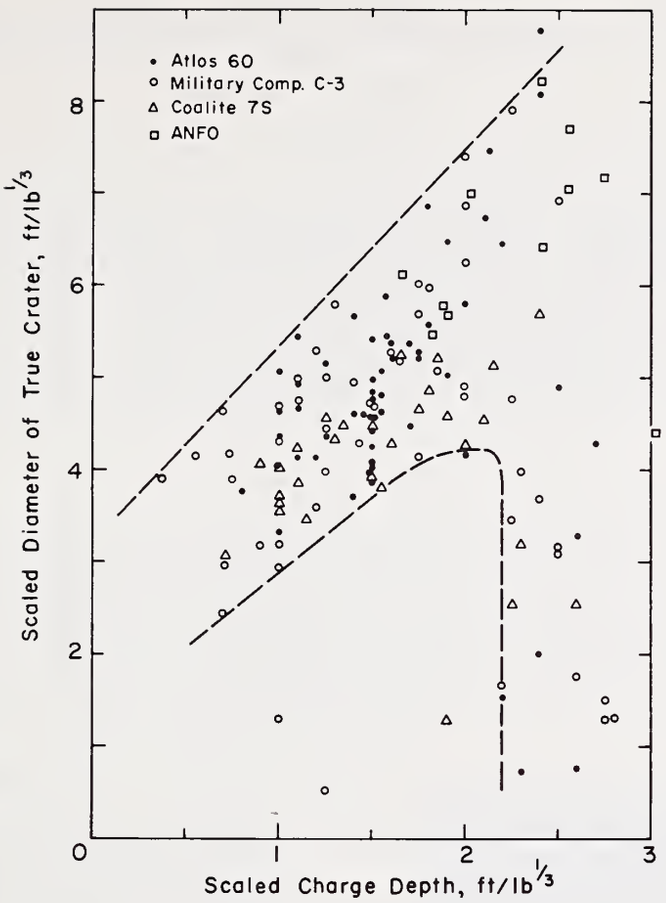

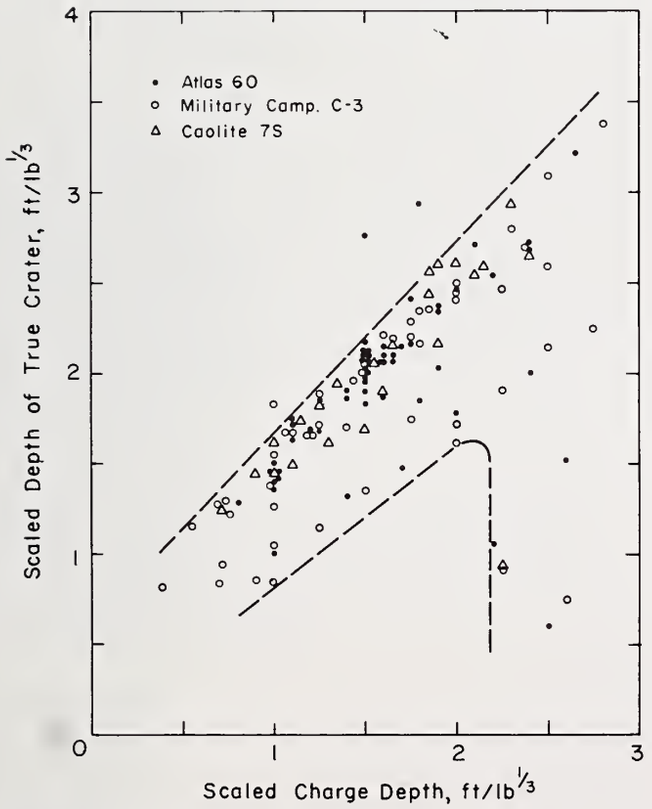

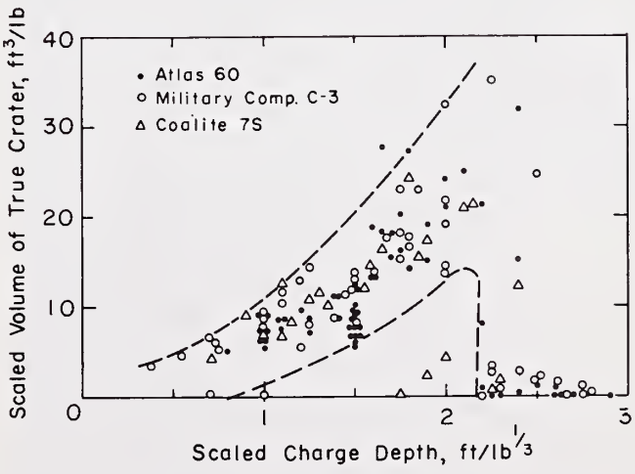

Figure A3. Scaled crater data for a frozen mixture of gravel and silt. (Basic data from Livingston and Murphy 1959, Mellor and Sellmann 1970.)

OBSERVATIONS OF AVALANCHE IMPACT PRESSURES[1]

P. A. Schaerer

ABSTRACT

Observations were made of impact pressures produced by well developed dry snow avalanches. The equipment is described and preliminary results of two years observations are summarized. There is a strong variation of pressure during the passage of an avalanche. The peak pressure, p, observed several times in one avalanche, can be expressed as $p = \rho v^2/2$ with v the apparent speed of the avalanche front and ρ the density of the deposited avalanche snow. The average pressure was found to be 0.3 p.

Introduction

Impact pressures due to snow avalanches influence the design of structures such as bridges and towers of powerlines, which are located in their potential path. The Division of Building Research of the National Research Council of Canada initiated observations of impact pressures with the objective of obtaining information concerning the characteristics of avalanches and the loads produced by them on structures. Studies were carried out at Rogers Pass, British Columbia, where numerous avalanche paths are easily accessible from the Trans Canada Highway.

Observation Site and Equipment

An avalanche path was selected where more than 10 avalanches occur every winter. The avalanches originate 2,100 m above sea level and fall over steep rock and a snow-filled gully to the observation site at 1,330 m. For 200 m above the measuring site, the avalanche track is a straight channel with an average incline of 33°.

Several load cells were mounted on a steel frame in the center of the track (fig. 1). The cells had a surface area of 645 mm^2 (1 $inch^2$). They were placed in cylindrical, streamlined steel holders, which, in turn, were mounted on a steel vertical beam. The beam had a width of 50.8 mm (2 in.) and so was a minor obstruction to the moving snow. Impact pressures were measured with strain transducers and recorded on a light beam oscillograph at a sheltered location.

Numerous difficulties and failures of equipment had to be overcome during the first 3 years before reliable observations were obtained. Between 1970 and 1972, however, impact pressures produced by several dry snow avalanches were recorded.

Figure 1.--Steel frame with two load cells.

[1]This paper is a contribution of the Division of Building Research of the National Research Council of Canada, and is published with the approval of the Director.

Characteristics of a Dry Snow Avalanche

Dry snow avalanches become a mixture of flowing and airborne powder snow when falling over steep and irregular terrain. Visual observations of moving and deposited avalanche snow indicated that the flowing part consists of an aggregate of particles that range between powder of size 0.1 mm to balls about 100 mm in diameter. The depth of the flowing snow could be estimated from traces on the side of gullies and from the height to which snow was pressed against tree trunks in avalanche tracks. Numerous observations of this depth were made in the Rogers Pass area, and it was found to be usually three to four times greater than that of avalanche snow after it came to rest. The bulk density of the flowing snow, therefore, can be assumed to be about 0.3 times the density of the deposited snow.

The speed of the avalanche was determined by timing the avalanche front as it moved over a known distance in front of the load cells. The speed of the avalanche front may not be equal to that of the flowing snow behind the front, but it was the only speed observation that was practical.

Recorded Impact Pressures

The number of pressure cells was limited and allowed the observation of the impact pressure of the dense, flowing part of the avalanche only to a height of about half its depth. Figure 2 shows the pressures observed during the passage of an avalanche.

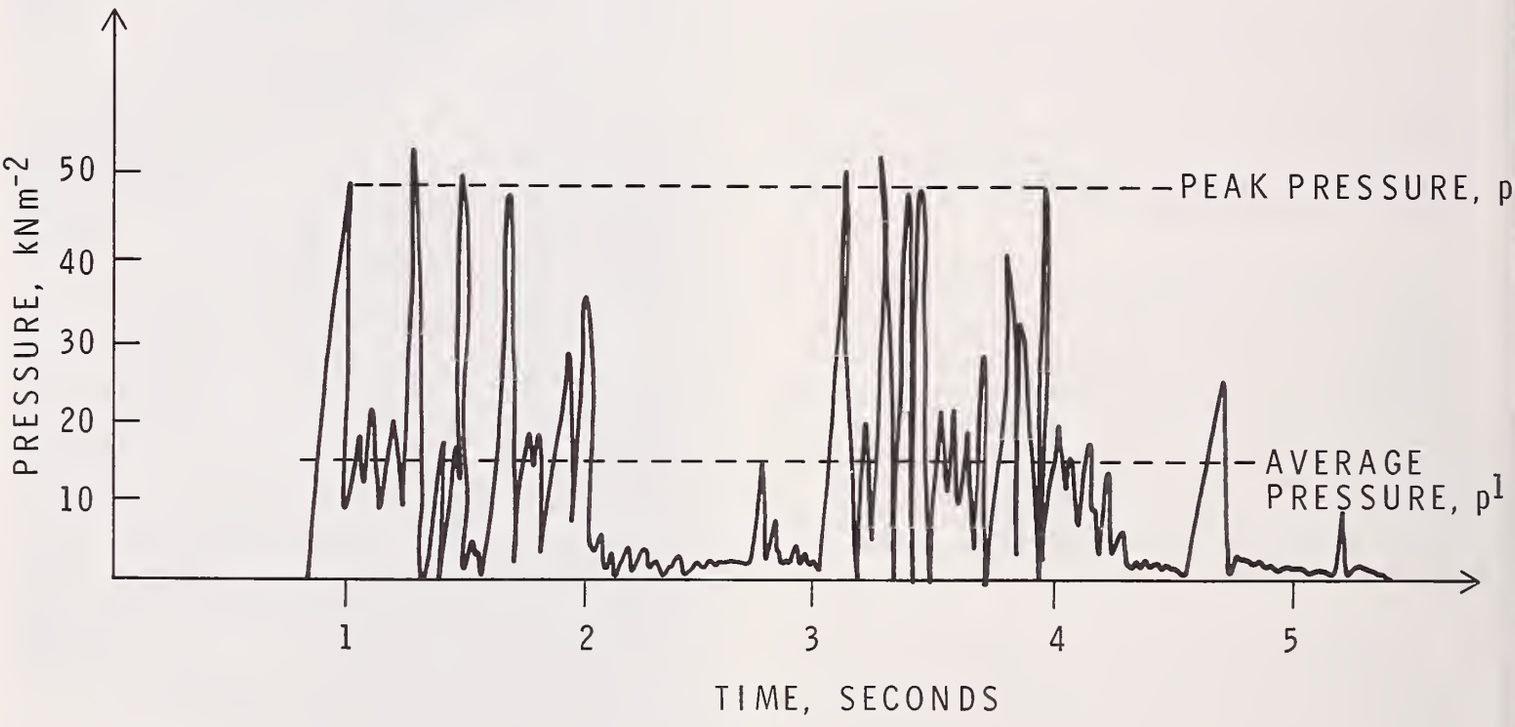

Figure 2.--Record of observed pressures.

Noteworthy is a series of pressure peaks with a duration of about 1 second and a recurrence period of about 2 seconds. They are probably the result of the complex nature of the start of the avalanches in irregular terrain. Snow would start to slide almost simultaneously at many places, but arrive at different times in the principal avalanche track, and, therefore, continue its motion in several mass waves. Recurring sets of peaks were not observed with minor avalanches that contained snow from only one small area of more or less uniform slope. Differences in particle size and bulk density are responsible for the fluctuations in pressure. Snowballs impinging on the load cells produced the peak pressures, and snowdust the low pressures.

A more uniform pressure with a small variation between extremes would probably be observed by using a cell with a larger measuring surface.

Analysis

The most advanced studies of avalanche dynamics are those by Salm (1967), Shen and Roper (1970), and Voellmy (1955). They considered the moving snow to be a compressible solid body or fluid.

If it is assumed that there is little compaction of the snow and little drag resistance associated with small obstacles, such as the load cells and the supporting frame used for the study, the impact pressure on unit surface area perpendicular to the flow can be expressed as:

$$p = \frac{v^2}{2} \rho$$

It was found that the observed peak pressures, p, agreed with the calculated pressures when v = the speed of the front of the avalanche, and ρ = the density of the deposited snow after the avalanche had stopped. (The density of the deposited snow would probably be equal to the density of large particles in the moving snow.)

The observed average pressure agreed with the calculated pressure

$$p = \frac{v^2}{2} \rho'$$

when ρ' was the average density of the following snow, or $\rho' = 0.3 \rho$. Values of observed peak and average pressures, and corresponding calculated values are presented in table I.

TABLE I

OBSERVED AND CALCULATED IMPACT PRESSURES

Date	Speed, v $m\ s^{-1}$	Density of Deposit, ρ $kg\ m^{-3}$	Peak Pressures p $kN\ m^{-2}$*		Average Pressure p' $kN\ m^{-2}$*		Depth of Flowing Snow m
			Observed	Calculated	Observed	Calculated	
7 Dec 1970	35.7	350	182	222	62	67	2.5
30 Dec 1970	53	310	256	435	105	131	1.8
16 Jan 1971	14.8	260	30	28	7.7	8.5	1.5
27 Jan 1971	14.7	225	35	24	8.3	7.2	0.9
30 Jan 1971	19.1	320	60	58	16	17.4	3.0
3 Dec 1971	21.6	210	33	49	11.0	14.7	1.5
6 Jan 1972	16.9	300	38	43	11.7	12.9	1.5
20 Jan 1972	18.5	280	48	48	13.8	14.4	1.2

* $1 kN\ m^{-2} = 0.145$ psi

Conclusions

The study indicates that for practical purposes the impact pressure produced by dry snow avalanches can be calculated from the speed of the avalanche front and the density of the deposited snow.

The observations were made on avalanches of relatively low speed with a small loading surface. In future studies it will be necessary to measure: (1) impact pressures on large surfaces; (2) impact pressures produced by avalanches with high speed; and (3) the distribution of the pressures over the full depth of avalanches.

Literature Cited

Salm, B.
1967. On non-uniform, steady flow of avalanching snow. Int. Assoc. Sci. Hydrol. [Gen. Assembly, Berne 1967] Publ. 79, p. 19-29.

Shen, H. W., and A. T. Roper.
1970. Dynamics of snow avalanche (with estimation for force on a bridge). Int. Assoc. Sci. Hydrol. Bull. 15(1):7-26.

Voellmy, A.
1955. Über die Zerstörungskraft von Lawinen. Schweizerische Bauzeitung, Zurich. Vol. 73, Nos. 12, 15, 16, 19, 37. 1955. [On the destructive force of avalanches. Transl. by U.S. Dep. Agric. For. Serv., Alta Avalanche Study Center, Transl. 2, 64 p. 1964.]

Perla, R. I. [Compiler].
1973. Advances in North American avalanche technology: 1972 symposium. USDA For. Serv. Gen. Tech. Rep. RM-3, 54 p. Rocky Mt. For. and Range Exp. Stn., Fort Collins, Colo. 80521.

Seven technical presentations, made in connection with the USDA Forest Service National Avalanche Training Program, discuss acoustic signals emitted by snow under stress, aspects of snow slab mechanics, use of explosives, and problems of avalanche dynamics.

Oxford: 384.1:111.784. **Keywords:** Avalanches, snow management.

Perla, R. I. [Compiler].
1973. Advances in North American avalanche technology: 1972 symposium. USDA For. Serv. Gen. Tech. Rep. RM-3, 54 p. Rocky Mt. For. and Range Exp. Stn., Fort Collins, Colo. 80521.

Seven technical presentations, made in connection with the USDA Forest Service National Avalanche Training Program, discuss acoustic signals emitted by snow under stress, aspects of snow slab mechanics, use of explosives, and problems of avalanche dynamics.

Oxford: 384.1:111.784. **Keywords:** Avalanches, snow management.

Perla, R. I. [Compiler].
1973. Advances in North American avalanche technology: 1972 symposium. USDA For. Serv. Gen. Tech. Rep. RM-3, 54 p. Rocky Mt. For. and Range Exp. Stn., Fort Collins, Colo. 80521.

Seven technical presentations, made in connection with the USDA Forest Service National Avalanche Training Program, discuss acoustic signals emitted by snow under stress, aspects of snow slab mechanics, use of explosives, and problems of avalanche dynamics.

Oxford: 384.1:111.784. **Keywords:** Avalanches, snow management.

Perla, R. I. [Compiler].
1973. Advances in North American avalanche technology: 1972 symposium. USDA For. Serv. Gen. Tech. Rep. RM-3, 54 p. Rocky Mt. For. and Range Exp. Stn., Fort Collins, Colo. 80521.

Seven technical presentations, made in connection with the USDA Forest Service National Avalanche Training Program, discuss acoustic signals emitted by snow under stress, aspects of snow slab mechanics, use of explosives, and problems of avalanche dynamics.

Oxford: 384.1:111.784. **Keywords:** Avalanches, snow management.

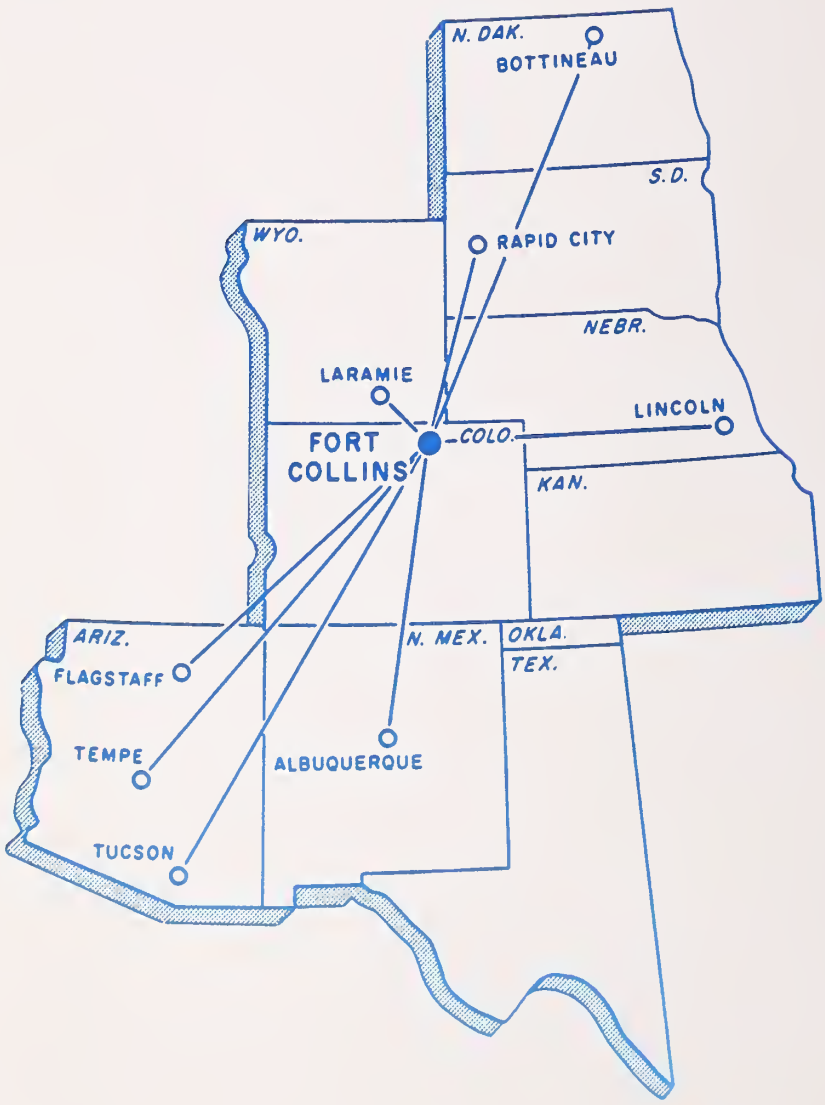
N. DAK.
BOTTINEAU
S.D.
WYO.
RAPID CITY
NEBR.
LARAMIE
LINCOLN
FORT
COLLINS
COLO.
KAN.
ARIZ.
N. MEX.
OKLA.
TEX.
FLAGSTAFF
TEMPE
ALBUQUERQUE
TUCSON